AD-A124 732 AN EXPERIMENTAL/ANALYTICAL INVESTIGATION INTO THE PERFORMANCE OF A 20-PER.. (U) AIR FORCE INST OF TECH WRIGHT-PATTERSON AFB OH SCHOOL OF ENGI.. J K HARVELL 1/1

UNCLASSIFIED DEC 82 AFIT/GAE/AA/82D-13 F/G 1/3 NL

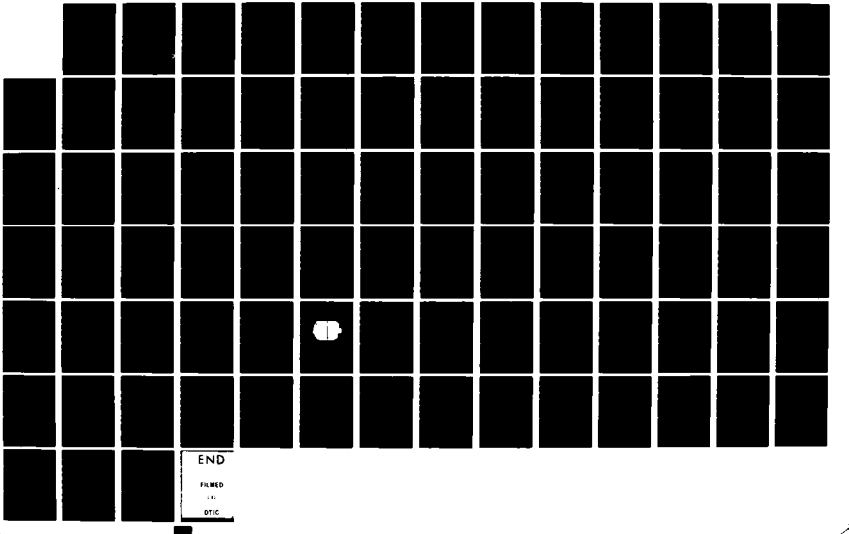

END

FILMED

DTIC

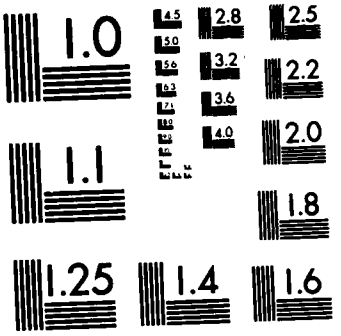

MICROCOPY RESOLUTION TEST CHART
NATIONAL BUREAU OF STANDARDS-1963-A

AN EXPERIMENTAL/ANALYTICAL INVESTIGATION INTO THE PERFORMANCE OF A 20-PERCENT THICK, 8.5-PERCENT CAMBERED, CIRCULATION CONTROLLED AIRFOIL

THESIS

AFIT/GAE/AA/82D-13 John K. Harvell
Capt USAF

DEPARTMENT OF THE AIR FORCE
AIR UNIVERSITY (ATC)
AIR FORCE INSTITUTE OF TECHNOLOGY

Wright-Patterson Air Force Base, Ohio

AFIT/GAE/AA/82D-13

AN EXPERIMENTAL/ANALYTICAL INVESTIGATION INTO THE PERFORMANCE OF A 20-PERCENT THICK, 8.5-PERCENT CAMBERED, CIRCULATION CONTROLLED AIRFOIL

THESIS

AFIT/GAE/AA/82D-13 John K. Harvell
Capt USAF

AFIT/GAE/AA/82D-13

AN EXPERIMENTAL/ANALYTICAL INVESTIGATION INTO THE PERFORMANCE OF A 20-PERCENT THICK, 8.5-PERCENT CAMBERED, CIRCULATION CONTROLLED AIRFOIL

THESIS

Presented to the Faculty of the School of Engineering
of the Air Force Institute of Technology
Air Training Command
in Partial Fulfillment of the
Requirements for the Degree of
Master of Science

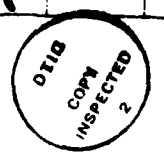

by
John K. Harvell, B.S.
Capt USAF
Graduate Aeronautical Engineering
December 1982

Acknowledgements

It is difficult to properly identify and reflect the considerable assistance I have received during completion of this thesis. To Dr Milton Franke, my advisor, I offer my sincerest appreciation for the insight, direction, and encouragement he provided during this investigation. To Majors Smith and Wallace, my thanks for faithfully serving on the thesis committee and their willingness to assist during difficult times. Mr Wales Whitt and Mr Nicholas Yardich, through their efforts installing instrumentation, and operating the tunnel provided friendship, assistance, and counsel during the numerous hours of experimental testing. Particular thanks to the AFIT shops for the skilled workmanship of Russ Murry and Dave Paine, whose eagerness and ability provided an avenue for successful construction and modification of the airfoil model. Thanks to Mr John Hicks and 4950th Test Wing Personnel for providing the use of their digitizer and instructing me in its use. To Ms Jane Abramson many thanks for the education she provided during our telephone conversations. To the technical photography section for the quick photographic processing and guidance in photographic procedures, thank you.

I will never be able to express adequately the contributions of my wife, Ginette, to the successful completion of this research. I most certainly would have

never finished without her encouragement, confidence, and devotion. For her many hours of perseverance while I bruised computer terminals and her unending support during moments of defeat, I pledge my continuing efforts in fulfillment of our mutual goals in life.

John K. Harvell

Contents

List of Figures

List of Tables

List of Symbols

a_j	Speed of sound at stagnation conditions, ft/sec
c	Airfoil chord length, ft
C_c	Section chordwise force coefficient
C_{d_o}	Section force drag coefficient
C_{d_r}	Section rake drag coefficient
C_{deq}	Section Equivalent Drag Coefficient
C_ℓ	Section lift coefficient
C_{m_o}	Section moment coefficient about leading edge
$C_{m_{25}}$	Section moment coefficient about quarter chord point
C_μ	Blowing momentum coefficient
C_n	Section normal force coefficient
C_p	Pressure coefficient
C_{p_d}	Section pressure drag coefficient
g_c	Conversion factor 32.174 $\frac{\text{lbm ft}}{\text{lbf sec}^2}$
h	Slot height
H	Shape factor of velocity profile
ℓ/d	Section lift-to-drag ratio
M	Mach number

$\dot{m}$	Mass rate of flow $\frac{\text{lbm}}{\text{ft sec}}$
P	Pressure, lbf/ft^2 (ABS)
q	Dynamic pressure, lbf/ft^2
R	Gas constant, 53.35 $\frac{\text{ft lbf}}{\text{lbm } ^\circ\text{R}}$
S	Airfoil span, ft
t	Airfoil thickness, ft
T	Temperature, °R
V	Velocity, ft/sec
x	Chordwise airfoil dimension, ft
y	Airfoil dimension normal to chord, ft
α_g	Geometric angle of attack, deg
γ	Ratio of specific heats
Λ	Shape factor of velocity profile in laminar boundary layer
Ø	Cylinder rotation angle, deg (Fig A-1)
DTNSRDC	David Taylor Naval Ship Research and Development Center

Subscripts

$(\ )_\infty$	Free stream conditions
$(\ )_{cp}$	Cylindrical plenum conditions
$(\ )_j$	Condition at jet location
$(\ )_\ell$	Lower surface location
$(\ )_{L.E.}$	Leading edge condition

$( )_{mp}$	Main plenum conditions
$( )_{sepl}$	Condition at lower surface separation
$( )_{sepu}$	Condition at upper surface separation
$( )_{T}$	Total conditions
$( )_{TE}$	Trailing edge condition
$( )_{LS}$	Local static condition
$( )_{FS}$	Freestream static condition

Abstract

This study was conducted to investigate the effect of two tangentially blown slots on the performance of a 20-percent thick, 8.5-percent cambered elliptical airfoil. Lift, drag, and moment coefficients were obtained at a test Reynolds number of 9.5×10^5 for secondary slot locations of 73.5 and 83.5 deg. Results show that the use of two tangentially blown slots enables the generation of higher lift coefficients at lower blowing rates. This feature enables the test airfoil to equal the performance of single slotted blown airfoils at lower blowing rates therefore reducing the parasitic losses and resulting in higher lift/drag ratios.

A limited study of the ability of the (TRACON) program to predict circulation controlled airfoil performance was conducted. The program failed to provide accurate predictions for the pressure distribution or force coefficients for the airfoil configuration of this study. This study also found that using different geometry smoothing techniques in the region of the slot resulted in large variations in TRACON's performance predictions. The obvious differences between the predicted pressure distribution and the experimental data, leads this author to the conclusion that (TRACON) is still in the developmental stages and should not be used as a design tool.

AN EXPERIMENTAL/ANALYTICAL INVESTIGATION INTO THE PERFORMANCE OF A 20-PERCENT THICK, 8.5-PERCENT CAMBERED, CIRCULATION CONTROLLED AIRFOIL

I. Introduction

During recent years, there has been considerable research conducted exploiting circulation control techniques in an effort to improve the short take-off and landing capabilities of military aircraft. Additional applications of circulation control techniques can result in heavy lift capability, special flight control characteristics, and reduced mechanical complexity in helicopter rotor mechanisms.

One of the more promising circulation control techniques takes advantage of the Coanda effect. The Coanda effect is basically described as the ability of a high speed jet to flow around a blunt edged surface without separation. This effect is primarily due to a balance between the centrifugal forces in the jet and the reduced pressure on the blunt surface (Ref 1). Circulation control airfoils take advantage of this effect by introducing a jet of high energy air into the suction surface trailing edge region of a blunt edged airfoil. Introduction of air at the lower blowing rates reenergizes the boundary layer thus enabling the suction surface flow to negotiate the airfoil's blunt

trailing edge without separation. This results in some lift recovery and a reduction in drag. When higher blowing rates are used, the additional energy in the jet forces the relocation of the trailing and leading edge stagnation points onto the lower surface of the airfoil. This movement of the stagnation points directly reflects the additional increase in lift produced by the higher blowing rates.

The advantages of this method become apparent when comparisons are made with conventional airfoil designs. First of all, conventional airfoils cannot produce the higher lift coefficients possible with blown airfoils due to the onset of flow separation. Secondly, where conventional airfoils require flaps and all their supporting control equipment to produce increases in lift, the blown airfoils are able to increase lift simply by regulating the mass flow rate of the blowing jet. Consequently there are considerable reductions in weight, complexity, and maintenance requirements for blown airfoils. The lift of blown airfoils is not strictly controlled by angle of attack variations. This uncoupled feature enables flight maneuvers not typical in conventional aircraft controls. With blown airfoil designs, an aircraft can be made to climb without varying the angle of attack. Additionally, pitching and rolling rates can be augmented by selective blowing.

Present disadvantages include first the problem of drag during cruise due to flow separation from the blunt trailing edge typical of blown airfoils; second, the parasitic drag

caused by energy requirements to produce the high energy air supply; and third, the large negative pitching moment caused by large suction peaks in the upper surface trailing edge region of blown airfoils.

Previous Research

Over the last 75 years, there has been considerable research into circulation control devices. A good summary of some of the works completed prior to 1961 is presented by Lachmann (Ref 2).

During the period from 1964-1967, Kind and Maul (Ref 3) were able to demonstrate lift coefficients as high as 3.3 using an uncambered, elliptical airfoil, thus identifying the potential of blowing as a circulation control technique. They pointed out that the drag was found to increase at about the same rate as the blowing momentum coefficient (C_μ). They concluded that the increased drag was due to large suction peaks in the trailing edge region of the airfoil and increased viscous losses due to mixing. Following some preliminary work, they postulated that one method of reducing the mixing losses, i.e. drag, was to use a splitter plate assembly.

Numerous studies (Refs 4-9) have been conducted investigating the effects of various trailing edge geometries and splitter plate configurations with splitter plates both fixed and free to rotate. This research showed

that reductions in mixing losses and drag are possible through the use of splitter plates.

During the same time frame, Williams and Howe (Ref 10), Englar (Ref 11-13), and Abramson (Ref 14,15) conducted extensive research into the factors influencing circulation controlled airfoil performance and their applications to fixed and rotary wing aircraft. Their research has resulted in a substantial base of information describing airfoil design criteria for strongly attached Coanda flow.

As a result of that research and considerable increases in airfoil performance Englar (Ref 16-18) modified and conducted preliminary tests on an A-6A aircraft demonstrating the short take-off and landing application of circulation controlled airfoils.

Whereas experimental investigation of circulation control techniques has progressed quite dramatically, theoretical evaluation of these devices has progressed quite slowly with only limited success. This difficulty in producing a theoretical model most likely stems from previous limitations in computational capability and difficulties modeling the complex nature of circulation control devices with a computational scheme which accurately describes the physics of the flow field. However, recent work by Dvorak (Ref 19) with the development of the TRACON program may present a method of investigating and optimizing circulation controlled airfoil designs prior to wind tunnel testing.

Present Study

When direct comparisons are made between blown and conventional airfoils, the drag measured during testing of the blown airfoils is generally modified by addition of the energy required to produce the high pressure air supplied to the blowing slot. The resulting term is identified as the equivalent drag. In addition, as pointed out by Kind and Maul and reinforced by numerous other works, drag generally increases as the blowing coefficient is increased. Subsequently, although continued increases in blowing rates have shown continued increases in lift, the penalties paid for that blowing become more severe.

The present study involves two main objectives. The first objective was to study the use of multiple tangentially blown slots in an elliptically shaped airfoil in an effort to produce high lift coefficients at low blowing rates. By accomplishing this task, the favorable characteristics of high lift are obtained at lower equivalent drag coefficients. By producing high lift at low blowing rates, the total pressure required in the plenum chambers is reduced. Therefore, the structural requirements for the plenum chambers can be relaxed somewhat resulting in additional weight reductions. The second objective of this study involves investigation of the ability of Dvorak's TRACON program to accurately predict solutions to flow around arbitrary two-dimensional geometries with blowing.

Scope

The first objective is accomplished in two phases. Phase one of this research involves the design, construction, and preliminary component testing of an airfoil incorporating two tangentially blown slots.

Phase two involves testing of the airfoil in the AFIT five-foot wind tunnel to determine whether two tangentially blown slots increases airfoil performance over that of a single blown slot.

The second objective of this study involves the use of the TRACON program. This includes acquiring the program, incorporating the program into the Aeronautical Systems Division computer, selecting appropriate test cases, and evaluating the results. Evaluation of this program does not include a rigorous disassembly and confirmation of the theoretical development, but is instead an evaluation of the ability of this code to predict solutions which coincide with experimental data.

II. Test Item Description and Instrumentation

Airfoil

The experimental model, Fig A-1, is a 20-percent thick, 8.5 percent cambered, elliptical airfoil with two tangentially blown slots. It incorporates the basic geometry of two models previously tested by Englar (Ref 1). The model has a span of 26 in, a chord length of 20.32 in and was designed such that the cylindrical trailing edge could be rotated to position the second blowing slot from zero to one hundred eighty degrees as desired.

The main plenum was constructed of 0.25 in aluminum (Fig A-2). Total pressure was measured in the main plenum by using five total pressure taps which were distributed spanwise to reflect any non-uniform conditions. A copper-constantan thermocouple was mounted on the plenum centerspan to measure plenum total temperature. Three dead stop and three tensioning screws, spaced evenly spanwise, were used to set the slot height (h) to 0.02 in. The location for the first blowing slot was fixed at 94.5 percent chord.

The brass circular trailing edge not only makes up the Coanda surface of the first slot, but also contains the second plenum and the entire second blowing slot. The second blowing slot was also 0.02 in in height and could be located arbitrarily by rotating the cylinder through the angle Ø (Fig A-1).

A total of sixty-seven static pressure taps were distributed along the centerspan of the model, twenty-seven on the suction surface, twenty-three on the pressure surface and seventeen on the circular trailing edge. Three static taps were located, 6 in to the right of centerspan and three 6 in to the left of centerspan. These additional taps were used to monitor the two-dimensionality of the flow field. Identification and location of the static pressure taps are shown in Table A-1. Additional model information and geometric considerations are described in Appendix A.

Wind Tunnel

Wind tunnel tests were performed in the AFIT five-foot wind tunnel at Wright-Patterson AFB. The AFIT five-foot wind tunnel is an open circuit, closed test section device with a maximum test speed of 200 miles per hour. The model and its location in the test section are shown in Fig A-3. Plywood ramps were used in the same fashion as that pointed out by Haupt (Ref 9) to produce a two-dimensional test environment.

In an attempt to reduce the downwash effects generated at the tips of an airfoil of finite span, large circular aluminum end plates were attached to both ends of the model. These plates were four feet in diameter, 0.22 in thick, and beveled 30 degrees at the edges. The combination of the plates and wind tunnel walls served to make a two-

dimensional test section, 26 by 60 in. The model was installed so as to span the tunnel vertically (Fig A-3) and was rigidly supported at each end. The air supplied to the main and cylindrical plenums was routed to the model through the upper and lower support members respectively. The geometric angle of attack (α_g) was fixed at zero throughout this investigation by orienting the model chord line so that it would coincide with the tunnel center line.

The turbulence factor of the tunnel is 1.5 (Ref 20) and accounts for the effect of the propeller, guide vanes, and tunnel wall vibrations. An effective Reynolds number, the product of the tunnel Reynolds number and the turbulence factor, should be used for comparison with flight tests or tests completed at other tunnel facilities.

The tunnel dynamic pressure "tunnel q" was maintained at 2.0 in of water (100 fps) throughout this test. Tunnel q was determined by comparing static pressure at the entrance to the test section with atmospheric pressure.

Flow Meters

Two 0.5 in throat diameter venturi meters were used to measure the mass flow rates to the model plenums. Static pressure readings were obtained at flange taps located at and immediately upstream of the venturi throat. The venturi meter used to measure the flow rate into the main plenum had been previously calibrated by the National Bureau of

Standards. The venturi meter used to measure the flow rate into the cylindrical plenum was calibrated by Rhynard (Ref 6). Temperature of the blowing air was measured with a copper-constantan thermocouple located upstream of the two venturi meters.

Wake Survey Rake

A wake survey rake was used to determine the momentum deficit in the wake of the airfoil. Ninety-four total head and six static tubes, distributed along the span of the rake, were used to measure the pressures in the airfoil wake. The rake was placed horizontally across the tunnel, perpendicular to the airfoil span, 30 in or 1.48 chord lengths behind the airfoil centerspan. The rake was positioned so that the wake reading generally appeared on the tubes which were spaced 0.25 in along the span.

Manometers

Sixty-eight tubes of an alcohol filled vertical manometer bank were used to measure static pressures on the airfoil surface. A 100 tube manometer bank, filled with merium oil and inclined at 30 degrees to the horizontal, was used to measure the wake survey rake pressures.

In general, 50 in U-tube mercury manometers were used to measure the upstream and throat pressures of the venturi meters feeding the main and cylindrical plenums. In

addition, 50 in U-tube water manometers were used to measure the main and cylindrical plenum total pressures. When higher mass flow rates and plenum total pressures were required, 60 in mercury manometers were used for mass flow measurements and 50 in U-tube mercury manometers were used for plenum total pressure measurements. All manometers were referenced to atmospheric pressure and consequently produced gage pressure readings.

III. Experimental Procedure

Prior to airfoil installation in the wind tunnel, the model spanwise total pressure distribution for each slot was monitored for the range of blowing coefficients used during this study. Additionally, tests were conducted to identify flow angularity/attachment, and slot height variations.

Following the airfoil installation and equipment setup, the model geometric angle of attack (α_g) was set to zero degrees by manually aligning the chord line with the wind tunnel centerline. The geometric angle of attack was not varied during this study. The trailing edge was initially oriented such that the second blowing slot was located at the 180 degree position. Following this preliminary setup, the model pressure tap numerical designations were checked and blockage/leak tests were conducted. The secondary air source plumbing was checked for leaks and the wake rake was checked for blockage, leaks, and correct tube designations. Without collecting data, several shakedown runs were completed to insure proper function of pressure sensors, flow meters, supporting control equipment and measurement systems.

Testing was conducted in three phases. During all phases of testing, the tunnel was operated at a dynamic pressure corresponding to a nominal speed of 100 fps. The main and cylinder plenum blowing rates were generally

controlled by setting an upstream venturi pressure for each plenum.

First, a set of baseline tests were conducted to determine the airfoil performance due to single slot blowing from the main plenum ($C_{\mu_{cp}} = 0.0$). During these baseline tests, the location of boundary layer separation was visually identified on the vertical manometer boards to identify the locations where application of second slot blowing would be most promising. Using the information gathered during the first phase of testing, phases two and three involved positioning the second blowing slot at cylinder rotation angles (Ø) of approximately 73.5 and 83.5 degrees respectively and generating a family of airfoil performance curves.

The tunnel was brought to operating speed and an initial blowing rate was set for the main plenum. Then, to generate one curve, the blowing rate for the cylindrical plenum was incremented from zero to 35 in of mercury in 5 in increments. At each of these conditions, the venturi and plenum pressures and temperatures were recorded, and the model and wake manometer boards were photographed. Having completed this sequence of tests, the main plenum blowing rate was adjusted by 5 in of mercury and a new sequence of tests were conducted to produce another set of airfoil performance curves.

Additionally the model was fitted with nylon tufts and a restricted tuft study was conducted to visually monitor

the air flow around the model. Throughout the study, repeat runs were conducted to verify the repeatability of test results.

IV. TRACON (A Numerical Analysis for Circulation Controlled Airfoils)

In the recent past, Dvorak and Choi (Ref 19) developed a numerical code named TRACON to be used as a design tool for circulation controlled devices. A brief overview of the calculation procedure (Fig 1) consists of the calculation of the viscous and potential flow solutions, their interactions, and the convergence criteria. TRACON has been designed to predict solutions to flow about arbitrary two-dimensional geometries, with or without single slot blowing, for Mach numbers ranging from zero into the transonic region.

Potential Flow Analysis

In the potential flow analysis, the exterior surface of the airfoil is mapped conformally onto the exterior of a unit circle. Then, by direct inversion, the external flow is mapped onto the interior of the circle so the entire flow field can be solved in a finite domain. This inversion of the flow field translates the singular condition in the velocity potential from infinity in the intermediate frame to the origin of the mapped plane. In order to remove this singularity a translated potential is introduced.

The transformed equation, with boundary conditions, is modeled using a finite-difference scheme incorporating

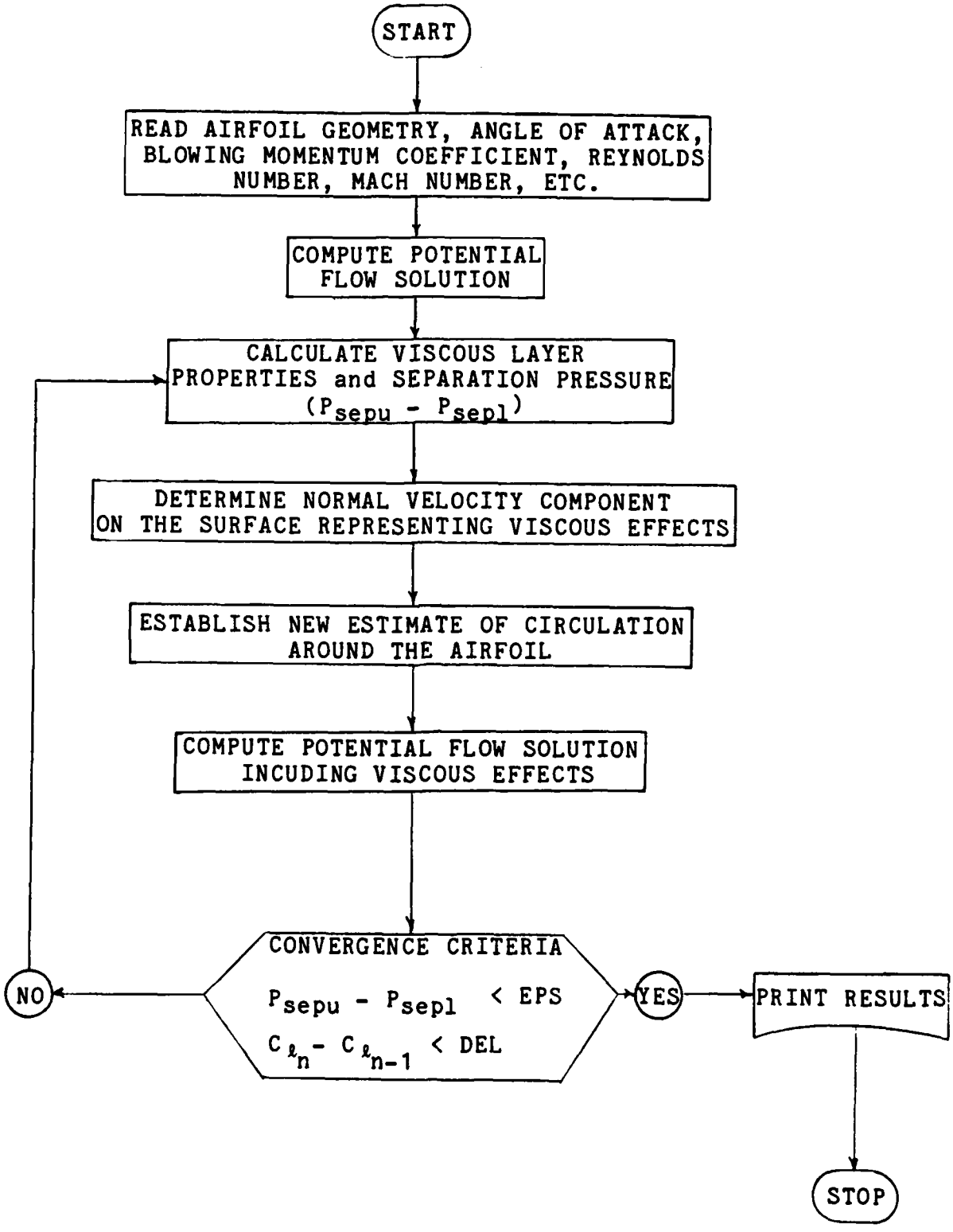

Fig 1. Calculation Procedure for TRACON Program

upwind differencing where the local flow is supersonic and central differencing at the subsonic points. The resulting set of difference equations are solved iteratively for the translated potential. Then the tangential velocity components on the surface of the airfoil can be obtained readily through simple differencing.

Boundary Layer Methods

The boundary layer development follows three distinctly different paths. First,the laminar boundary layer development is handled by the integral method of Cohen and Reshotko. The resulting integration formula is solved by trapezoidal rule. Then the momentum thickness and shape factor are obtained. Separation of the boundary layer is detected by examining the Pohlhousen parameter, with the assumption that the H-Λ table for the incompressible flow is still valid.

Following transition, Green's lag-entrainment integral method is used for the turbulent boundary layer development. This integral method involves the use of three equations, momentum-integral, entrainment, and a rate equation for the entrainment coefficient. This system of equations is solved using a Runge-Kutta method. The separation point can then be located by monitoring the friction coefficient and shape factor. The region of the blowing slot is treated by using a Crank-Nicolson type of finite difference scheme. The

calculations in this area are biased somewhat by the use of experimental information describing the pressure jump across the wall jet which is based on the results of Kind and the DTNSRDC.

Viscous-Potential Flow Interaction and Convergence Criteria

To initiate the procedure an initial value of circulation is assumed. The initial viscous and potential flow solutions are then calculated and the convergence criteria are checked. If the convergence criteria are not met, the effect of the viscous layer is incorporated into the airfoil geometry through the addition of a boundary layer displacement thickness parameter. This results in new viscous and potential flow solutions and this cycle is continued until the convergence criteria are met. The convergence criteria are satisfied when the lift coefficients remain essentially unchanged between iterations and the upper and lower surface separation pressures are equal.

The lift and pitching moment coefficients are obtained from the calculated pressure distribution, and drag is determined through direct integration of the skin friction and pressure around the airfoil contour.

A more complete treatment of the calculation procedure, including equations, assumptions, test results, and user instructions, can be found in Ref 19.

V. Data Reduction

The data recorded during wind tunnel testing were reduced to five principal coefficients. Those five coefficients include the momentum coefficient, the section lift coefficient, the section quarter chord moment coefficient, the section pressure drag coefficient, and the section drag coefficient. The model and wake manometer displacements, recorded on photographic negatives, were digitized using a Triad Corporation V/R 100 c/m film reader. Following determination of these coefficients, the lift to drag ratio and section lift augmentation ratios were also calculated.

Momentum Coefficient

The momentum coefficient (C_μ) is defined as the momentum in the jet issuing from the slot nondimensionalized by division of the free stream dynamic pressure and airfoil chord length:

$$C_\mu = \frac{\dot{m}V_j}{q_\infty c}$$

The jet velocity in the slot exit plane is generally calculated by assuming isentropic expansion from plenum total pressure. The generation of the jet velocity equation starts with the following two relations:

$$\frac{P_T}{P_j} = \left(1 + \frac{\gamma-1}{2} M_j^2\right)^{\frac{\gamma}{\gamma-1}}; \quad M_j^2 = \frac{V_j^2}{a_j^2} = \frac{V_j^2}{\gamma R T_j g_c}$$

By the simple substitution and algebraic manipulation the jet velocity at the slot is found to be

$$V_j = \left[2RT_T\, g_c \left(\frac{\gamma}{\gamma-1}\right) \left(1 - (P_j/P_T)^{\frac{\gamma-1}{\gamma}}\right)\right]^{1/2}$$

It should be noted that the development of V_j shown here requires that the isentropic expansion be from plenum total pressure to local static pressure in the slot exit plane. However, as pointed out by Englar (Ref 1), the momentum coefficient is generally calculated using expansion from plenum total pressure to free stream static pressure in an effort to reduce the effects of model orientation and geometry.

Because of the volume of data using expansion to free stream static pressure, the results of this study use this criteria in order to facilitate comparison. However, due to the potentially large variation in momentum coefficients calculated by these two methods, conversion curves are presented to enable calculation of the momentum coefficient based on expansion to local static pressure.

Since the model contained two blowing slots, two independent momentum coefficients were calculated. The main

and cylindrical plenum momentum coefficients were symbolized by $C_{\mu_{mp}}$ and $C_{\mu_{cp}}$ respectively. Then a total momentum coefficient was defined as the summation of the main and cylindrical plenum momentum coefficients as shown below:

$$C_{\mu_T} = C_{\mu_{mp}} + C_{\mu_{cp}}$$

Section Lift and Pressure Drag Coefficient

The section normal and chordwise force coefficients were calculated by integrating the static pressure distribution over the upper/lower and leading/trailing edge surfaces of the model respectively. These integrals were calculated by fitting smooth cubic splines through the experimental data points and then integrating those spline curves using cubic spline quadratures. The functional form of the relations used to calculate these coefficients are as follows:

$$C_n = \int_0^1 (C_{p_\ell} - C_{p_u}) d\left(\frac{x}{c}\right)$$

$$C_c = \int_{-t/2c}^{t/2c} (C_{p_{LE}} - C_{p_{TE}}) d\left(\frac{y}{c}\right)$$

where $\left(\frac{x}{c}\right)$ and $\left(\frac{y}{c}\right)$ are the non-dimensional distances along and perpendicular to the chord line respectively.

Section lift and pressure drag coefficients were then computed using the folowing relations:

$$C_\ell = C_n \cos \alpha_g - C_c \sin \alpha_g$$

$$C_{p_d} = C_n \sin \alpha_g + C_c \cos \alpha_g$$

where α_g is the geometric angle of attack.

Section Moment Coefficient

The section quarter chord moment coefficient ($C_{m_{25}}$) was calculated in two steps. First the section moment coefficient about the leading edge was calculated using the following relation:

$$C_{m_o} = \int_0^1 (C_{p_\ell} - C_{p_u}) \times d\left(\frac{x}{c}\right) + \int_{\frac{-t}{2c}}^{\frac{t}{2c}} (C_{p_{LE}} - C_{p_{TE}}) \, y \, d\left(\frac{y}{c}\right)$$

Where the first term on the right accounts for the moment due to lift producing forces distributed over the upper and lower surfaces and the second term accounts for the moment due to pressure drag forces distributed over the leading and trailing edges.

Then the quarter chord moment coefficient was calculated using the folowing relation:

$$C_{m_{25}} = C_{m_o} + C_\ell/4$$

Section Drag Coefficient

The momentum deficit method of Betz and Jones (Ref 21) enables calculation of friction and pressure drag (i.e., profile drag) coefficients. The simple form of this equation, presented in Pope (Ref 20), allows calculation of the profile drag coefficient by resolving the free stream and wake static and total pressures. The functional form of the equation used to calculate the section rake drag coefficient is shown below:

$$C_{d_r} = 2 \int_0^1 \left(\sqrt{\frac{q}{q_\infty}} - \frac{q}{q_\infty}\right) d\left(\frac{x}{c}\right)$$

The development of this equation does not account for the additional momentum introduced at the blowing slot. Therefore, Englar (Ref 12) introduced a modification to the section rake drag coefficient. This modification involved subtracting the non-dimensional component of momentum introduced at the blowing slot from the section rake drag coefficient, thus producing the section force drag coefficient as shown below:

$$C_{d_o} = C_{d_r} - \frac{\dot{m} V_\infty}{q_\infty c} = C_{d_r} - C_\mu \frac{V_\infty}{V_j}$$

To facilitate comparison of circulation controlled airfoil performance with that of conventional airfoils, the section force drag coefficient was modified by the addition of the power required to produce the high pressure air supplied to the blowing slot (Englar, Ref 12). This results in a term called the section equivalent drag coefficient which is defined below:

$$C_{d_{eq}} = C_{d_o} + C_\mu \frac{V_j}{2V_\infty} + C_\mu \frac{V_\infty}{V_j}$$

The second term on the right represents the power required to compress the inlet air from free stream static pressure to the pressure supplied to the plenum. The third term represents the ram drag effect caused when air used in blowing enters the aircraft engine.

As described by Pajayakrit (Ref 22), the total momentum coefficient may not accurately account for the price of blowing. Therefore the section force drag and section equivalent drag coefficients were calculated in the following fashion for this study:

$$C_{d_o} = C_{d_r} - C_{\mu_{mp}} \frac{V_\infty}{V_{jmp}} - C_{\mu_{cp}} \frac{V_\infty}{V_{jcp}}$$

$$C_{d_{eq}} = C_{d_o} + C_{\mu_{mp}} \left(\frac{V_{jmp}}{2V_\infty} + \frac{V_\infty}{V_{jmp}} \right) + C_{\mu_{cp}} \left(\frac{V_{jcp}}{2V_\infty} + \frac{V_\infty}{V_{jcp}} \right)$$

This method accounts for the individual penalty generated by each blowing slot. For this study, the lift to drag ratio was calculated using the section equivalent drag coefficients.

Wind Tunnel Corrections

Boundaries in the wind tunnel test section and model/wake interference generally cause minor errors in the reduced data. Subsequently, corrections are made to improve the accuracy of the reported data. The standard corrections suggested by Pope (Ref 20) for solid blockage, wake blockage, and streamline curvature were applied to lift/moment coefficients. Solid and wake blockage corrections were used to adjust drag, free stream velocity, dynamic pressure, and Reynolds number.

Other errors are introduced into this data (ie, measurement, digitizing, and roundoff) but are generally of a minor nature. For further explanation of the description and magnitude of these measurement/reduction errors refer to Pajayakrit (Ref 22).

VI. Results and Discussion

Preliminary Study

Previous research by Haupt (Ref 9) and Pajayakrit (Ref 22) identified two problems of considerable consequence in producing uniform two-dimensional flow with good Coanda attachment. The first of these is the requirement to produce uniform flow across the span at the slot exit plane with minimal spanwise flow. Second, that the main requirement for good Coanda jet attachment is that the jet must be tangent to the downstream surface of the airfoil at the slot exit plane. As these features are critical for good airfoil performance, the model used in this study was bench tested prior to installation in the tunnel to insure that it met these criteria. This preliminary study showed that the spanwise pressure distribution was uniform within a few percent, and a limited tuft study indicated that there was no noticeable spanwise flow. Although stiffening screws reduced the magnitude of the slot deflection it was noted that there was approximately 0.001 in expansion of the slot at the higher blowing rates. This slot expansion was basically uniform across the span and was not used to modify the blowing momentum coefficient. The preliminary study did indicate good flow attachment in the trailing edge region of the model.

General Observations

Initial test runs with no blowing indicated that there was a two-dimensional flow field present. The static pressure readings for the airfoil surface indicated that there was a local favorable pressure gradient just downstream of the slot exit plane. This was a feature designed into the airfoil to improve the likelihood of good jet attachment. When no blowing was used it was evident that the majority of the trailing edge region of the airfoil was separated.

The baseline tests (tests with single slot blowing from the main plenum only) demonstrated good Coanda attachment, a two-dimensional test section, and obvious increases in section lift coefficient. During the baseline tests, the static pressure readings for the airfoil indicated that the Coanda jet separated from the trailing edge for angles (Ø) ranging from 70 to 90 deg depending upon the blowing momentum coefficient. Due to the location of jet separation, cylinder rotation angles of Ø = 73.5, 83.5, and 93.5 were chosen for further study.

During tests incorporating blowing from both slots, it was apparent that there were considerable increases in lift. However, at the higher blowing rates there was some degradation of the two-dimensionality of the flow field. It is expected that this was caused by vortices, generated by flow interference with the model sideplates, inducing a

downwash on the model. This condition was only apparent in the high lift situations. The research done at DTNSRDC has incorporated tip jets to reduce this interference effect with quite good results. Unfortunately limitations in the available secondary air supply prevented using this technique during this study.

When both blowing slots were used, the static pressure readings for the model indicated Coanda jet turning angles of as much as 150 degrees. It is expected that this value would be increased with the use of an improved design for the second blowing slot slot (Fig A-4) or increased blowing momentum coefficients. During some test cases involving low main plenum blowing coefficients, there was some fluctuation in the model static pressure indications. It is believed that testing in this region indicates the transition between flow attachment and flow separation points prior to the second blowing slot. A brief sequence of preliminary tests with the second slot located at 93.5 deg indicated a failure to keep the flow attached up to the second blowing slot except at the higher main plenum blowing momentum coefficient. Due to limitations in the amount of secondary air available this test condition was not investigated further. Due to the preliminary nature of these tests and the failure of the flow to remain attached, the model and wake pressure indications were visually monitored rather than recorded and reduced. Consequently no reduced data is presented for this configuration.

The flow visualization study conducted in the wind tunnel indicated two-dimensional flow over the airfoil. Reinforcing the previously identified results, the tuft study showed flow separation in the trailing edge region of the airfoil for the no blowing case, and progressive flow attachment as blowing was increased. The tufts showed that there was uniform spanwise flow attachment in trailing edge region without any apparent vortices.

Lift Results

The lift results are presented in Figs B-1 and B-2 as section lift coefficients (C_ℓ) versus total momentum coefficient (C_{μ_T}). For comparative purposes the baseline curve n ($C_{\mu_{cp}} = 0.000$) is repeated in each figure. The curves reflect quite dramatically the advantage the dual slot configuration provides over the single slot configuration. For example, lift results for $\emptyset = 73.5$ deg, show that there is a 28 to 50 percent increase in section lift coefficient for a total momentum coefficient of 0.05 depending upon $C_{\mu_{mp}}$. The slope of the curves indicating two blowing slots approaches the slope indicated in the single slot blowing case at the higher momentum coefficients. However, it is apparent that using the dual blowing slot results in higher lift coefficients than the single blowing slot configuration for equivalent total momentum coefficients. The second feature that should be pointed out is

that the better lift curves are generated for the lower main plenum blowing momentum coefficients. That is, once the main plenum blowing has provided the energy required to keep the boundary layer attached up to the second blowing slot, any additional main plenum blowing does not increase lift as much as that for the same additional amount of blowing at the second blowing slot. When the main plenum blowing momentum coefficient was below that required for boundary layer attachment up to the second slot, blowing provided at the second slot resulted in lift coefficients that are lower than those obtained with single slot blowing at equivalent total momentum coefficients. The results of this condition are seen when comparisons are made between the * ($C_{\mu_{mp}}$ = 0.000) and + ($C_{\mu_{mp}}$ = 0.0074) curves and the baseline n ($C_{\mu_{cp}}$ = 0.000) curve of Fig B-1. The + and * curves of (Fig B-1) are terminated due to an audible model resonance experienced at the next test condition for each curve. The cause of this resonance was not investigated during this study. Comparisons between the two test configurations are a bit more subtle. When the cylinder rotation angle (Ø) was set at 83.5 deg there was a requirement for slightly higher main plenum blowing momentum coefficients to keep the boundary layer attached up to the second blowing slot. However, this was offset somewhat by the increased ability of the second blowing slot to produce lift increases, due to its position farther around the trailing edge. Direct comparison of Figs B-1 and B-2 show

that dual slot blowing at both cylinder rotation angles (Ø) result in similiar lift coefficient curves and neither configuration shows higher lift coefficients than the other at comparable conditions.

An additional feature which is presented by this design is the ability to place the first blowing slot a little farther forward, chordwise, without paying a large penalty in performance. This feature enables the airfoil to operate over an expanded range of angles of attack without inducing boundary layer separation before the first blowing slot. It is noted here that it may be possible to produce even higher lift coefficients (C_ℓ) at the same total momentum coefficient (C_{μ_T}) by introducing a third slot in the same fashion as the second.

Lift augmentation curves representing the effect of blowing are shown in Figs B-3 and B-4. These curves differ somewhat from the conventional single slot configurations in that the peak values of lift augmentation occur at values other than those close to the origin of the blowing momentum coefficient. The reason for this difference is that the starting points of the curves depicting dual slot blowing are offset along the C_{μ_T} axis by the main plenum blowing momentum coefficient used for each respective test configuration. Comparisons of Figs B-3 and B-4 show that the $x(C_{\mu_{mp}} = 0.0171)$ curve of Fig B-4 reflects the highest lift augmentation ratio. A second result is that the peak

values of Lift Augmentation for the Ø = 83.5 deg curves are at higher C_{μ_T}'s than the curves at Ø = 73.5 deg.

Pressure Drag and Moment Results

Pressure drag results are presented in Figs B-5 and B-6 as section pressure drag coefficient (C_{p_d}) versus total momentum coefficient (C_{μ_T}). Care should be taken when drawing conclusions from these curves as they only depict static conditions on the airfoil surface. They do not contain any potential thrust terms which may be present due to expansion of the jet from plenum total pressure to local static pressure. However, they do represent quite graphically the pressure on the exterior of the airfoil resulting from the suction peak generated by the Coanda effect. The pressure drag results presented in Figs B-5 and B-6 show a distinct difference between the single slot (n) and dual slot configurations. The dual slot configurations result in higher pressure drag coefficients because the low pressure zone caused by the Coanda effect is located farther around the trailing edge of the airfoil. Comparisons of Figs B-5 and B-6 show that the 83.5 deg cylinder rotation angle resulted in higher pressure drag coefficients than the Ø = 73.5 deg condition.

The moment results are presented in Figs B-7 and B-8 as section quarter chord moment coefficient (C_{m25}) versus total momentum coefficient (C_{μ_T}). These curves highlight one of the continuing difficulties of the circulation controlled

airfoils. The Coanda effect produces substantial suction in the upper surface trailing edge of the airfoil which produces the favorable effects of high lift. However, at the same time, this concentration of lift producing forces in the aft section of the airfoil causes a severe nosedown pitching moment. As a consequence, when using these devices in conventional aircraft applications, care must be taken to redesign the horizontal stabilizer to offset this pitching moment (Ref 16). Unfortunately, this feature is a direct result of the fundamental nature of this circulation control technique and as such it is unlikely that it will be eliminated. As would be expected, the generation of higher lift coefficients results in a more severe nosedown pitching moment. As seen in Figs B-7 and B-8, the dual slot configurations result in more severe nosedown pitching moments than the single slot (n) configuration at equivalent total momentum coefficients. Comparisons between Figs B-7 and B-8 show that the nosedown pitching moments of the dual slot configurations are of the same magnitude.

Drag Results

Equivalent drag results are presented in Figs B-9 and B-10 as section equivalent drag (C_{deq}) versus total momentum coefficient (C_{μ_T}). However, before any comment is made about these results, a few qualifying statments must be made.

Although all the modifications to the measured (i.e., Rake Drag Coefficient) drag follow quite naturally from the development, the corrections are in some cases an order of magnitude larger than the actual measured drag. As a result, the basis for calculation of the blowing momentum coefficient is of particular concern as this parameter is a primary component of the corrections. As shown in Figs B-11 and B-12 the difference in blowing momentum coefficients based on calculations using expansion to freestream vs local static pressure can introduce variations in this coefficient of 25 percent or more. These types of variations will have considerable effect on both the equivalent drag term and the lift/equivalent drag ratio.

A second problem is that pointed out by Pope (Ref 20) in his explanation of the use of a wake rake and the momentum deficit method in general. Pope states that the wake rake when used with the momentum deficit method is only accurate when measuring drag on an airfoil which is not stalled. His explanation is that the previously stated method only resolves the linear variation in momentum and that in the case of separated flow there are significant losses of a rotational nature. At the higher blowing rates, there is enough energy in the jet to enable the upper surface trailing edge flow to turn around the majority of the trailing edge and impinge upon the lower surface free stream flow. Under these conditions there are considerable

changes in linear momentum but there are also undoubtedly considerable rotational effects. An additional note is that a wake rake, used in conjunction with a manometer bank, is a time averaging device. As a consequence any unsteady condition in the region of the wake is essentially lost and readings of a cyclic behavior may be affected by the response time of the system. One final word of caution is that drag results have been reported in numerous ways in other references so care must be taken comparing results from different sources.

Given these qualifications, the drag of the single slot configuration is seen to be slightly greater than the dual slot configurations at equivalent total momentum coefficients (Figs B-9 and B-10). Additionally, Figs B-13 and B-14 show the distinct advantage of the dual slot configurations over the single slot configuration. By using the dual slot configurations, higher lift to equivalent drag ratios are obtained for a much wider range of lift coefficients. Comparison of Figs B-13 and B-14 show that the $x(C_{\mu_{mp}} = 0.0171)$ curve for the 83.5 deg cylinder rotation angle results in lift to drag ratios superior to any other configuration tested.

TRACON

The potential flow solution technique, being a conformal mapping, eliminates the ability to model the test

airfoil without smoothing the geometry in the region of the slot. Unfortunately there is no guidance in the program documentation explaining a concise repeatable method whereby two independent parties would generate the same geometric smoothing. For this reason a number of different methods were used in an attempt to produce a smooth geometry in the region of the slot. Then each of these test cases were run to determine how sensitive the program was to minor geometric changes in the region of the slot. The results of these test cases are compared with the baseline experimental data in Figs B-15 to B-17.

These results identify considerable differences between the experimental results and the computational results of TRACON. They also show that small differences in the geometry smoothing in the region of the slot can result in large variations in the computer solution. One of the items of particular concern was that the moment results predicted by TRACON indicate a nose up, i.e., positive, pitching moment which is contrary to all experimental data on circulation controlled airfoils.

When a closer look was taken at the codes generation of the airfoil's pressure distribution it was noted that the pressure distribution reflected a substantial leading edge suction peak and a relatively mild trailing edge suction peak. This pressure distribution is quite different from that obtained in the experimental work. For these reasons it is felt that this program is still in the developmental stages and should not presently be used as a design tool.

VII. Conclusions and Recommendations

This experimental/analytical investigation of a two-dimensional circulation controlled airfoil resulted in the following conclusions:

1. The airfoil using two blowing slots produced higher overall C_ℓ and $C_\ell/C_{d_{eq}}$ then the same airfoil using single slot blowing alone for the same C_{μ_T}.

2. When using two slots, maximum $C_\ell/C_{d_{eq}}$ can be obtained by limiting the blowing from the primary slot to just the amount needed to insure good flow attachment up to the secondary slot.

3. TRACON did not accurately predict pressure distributions or force coefficients for the airfoil of this study.

It is recommended that studies be conducted:

1. to investige the effect of the proposed improvements to the second plenum for a range of angles of attack and tunnel dynamic pressures.

2. to investigate the possibility of an optimum secondary slot rotation angle (Ø).

3. to investigate whether using three tangentially blown slots will allow for generation of higher lift coefficients at even lower momentum coefficients.

4. to examine the computational procedure of TRACON, identify potential difficulties, limitations, and provide improvements where possible.

5. to develop a geometry smoothing technique in the region of the slot that results in repeatable/acceptable solutions regardless of airfoil geometry.

Bibliography

1. Englar, R. J. Experimental Investigation of the High Velocity Coanda Wall Jet Applied to Bluff Trailing Edge Circulation Control Airfoils. NSRDC Technical Report - 4708, Bethesda, MD: Naval Ship Research and Development Center, September 1975.

2. Lachmann, G. V., Editor. Boundary Layer and Flow Control. Vols I and II. New York: Pergamon Press, 1961.

3. Kind, R. J. and D. J. Maull. "An Experimental Investigation of a Low-Speed Circulation-Controlled Aerofoil," The Aeronautical Quarterly, 19: 170-182 (May 1968).

4. Stevenson, Thomas A. "A Wind Tunnel Study of the Lift-Drag Ratio on a Cambered Circulation Controlled Airfoil," Unpublished Master's Thesis, Wright-Patterson AFB, OH: Air Force Institute of Technology, June 1974.

5. Stevenson, Thomas A. et al. "Wind Tunnel Study of a Circulation-Controlled Elliptical Airfoil," Journal of Aircraft, 14: 881-885 (September 1977).

6. Rhynard, Wayne E. "A Wind Tunnel Study of the Effects of Splitter Plate Position and Angle on the Lift-Drag Ratio of a Circulation Controlled Elliptical Airfoil," Unpublished Master's Thesis, Wright-Patterson AFB, OH: Air Force Institute of Technology, October 1974.

7. deJonckhere, Richard K. "An Analytical and Experimental Study of the Effects of Splitter Plate Position on the Trailing Edge Modifications of a Cambered Circulation Controlled Elliptical Airfoil," Unpublished Master's Thesis. Wright-Patterson AFB, Ohio: Air Force Institute of Technology, December 1975.

8. Oxford, Vail S. "A Wind Tunnel Study of the Effects of Trailing Edge Modifications on the Lift-Drag Ratio of a Circulation Controlled Airfoil," Unpublished Master's Thesis, Wright-Patterson AFB, OH: Air Force Institute of Technology, December 1975.

9. Haupt, Stuart L. "An Experimental and Analytical Investigation into the Effects of a Freely Rotating Splitter Plate on the Performance of a Circulation Controlled Airfoil," Unpublished Master's Thesis, Wright-Patterson AFB, OH: Air Force Institute of Technology, December 1980.

10. Williams, R. M. and H. J. Howe. Two-Dimensional Subsonic Wind Tunnel Tests on a 20-Percent Thick, 5-Percent Cambered Circulation Control Airfoil. NSRDC Technical Note Al-176. Bethesda, MD: Naval Ship Research and Development Center, August 1970.

11. Englar, R. J. Two-Dimensional Subsonic Wind Tunnel Tests of Two 15-Percent Thick Circulation Control Airfoils. DTNSRDC Technical Note AL-211. Bethesda, MD: David Taylor Naval Ship Research and Development Center, August 1971.

12. Englar, R. J. Two-Dimensional Subsonic Wind Tunnel Investigations of a Cambered 30-Percent Thick Circulation Control Airfoil. NSRDC Technical Note AL-201, Bethesda, MD: Naval Ship Research and Development Center, May 1972.

13. Englar, R. J. Subsonic Two-Dimensional Wind Tunnel Investigations of the High Lift Capability of Circulation Control Wing Sections. DTNSRDC Technical Report ASED-274. Bethesda, MD: David Taylor Naval Ship Research and Development Center, April 1975.

14. Abramson, J. Two-Dimensional Subsonic Wind Tunnel Evaluation of a 20-Percent Thick Circulation Control Airfoil. DTNSRDC ASED-311, Bethesda, MD: David Taylor Naval Ship Research and Development Center, Code 1619, June 1975.

15. Abramson, J. Two-dimensional Subsonic Wind Tunnel Evaluation of Two Related Cambered 15-Percent Thick Circulation Control Airfoils, DTNSRDC ASED-373, Bethesda, MD: David Taylor Naval Ship Research and Development Center, Aviation and Surface Effects Department, September 1977.

16. Englar, R. J. Development of the A-6/Circulation Control Wing Flight Demonstrator Configuration, DTNSRDC Technical Report ASED-79/01. Bethesda, MD: David Taylor Naval Ship Research and Development Center, January 1979.

17. Mayfield, J. Circulation Control Wing Demonstrates Greater Lift, Aviation Week and Space Technology, March 19, 1979.

18. Englar, R. J., Nichols, J. H., Harris, M. J., and Huson, G. "Experimental Development of an Advanced Circulation Control Wing System for Navy STOL Aircraft". AIAA 19th Aerospace Sciences Meeting, Paper AIAA-81-0151, St Louis, Missouri, January 1981.

19. Dvorak, F. A. "The Development of an Analytic Method for Two-Dimensional Circulation-Control Airfoils in Transonic Flow," Analytical Methods Report NO. 8106. Bellevue, Washington: Analytical Methods, Inc., June 1981.

20. Pope, A. Wind Tunnel Testing. New York: John Wiley and Sons, Inc., 1954.

21. Schlichting, H. Boundary Layer Theory (7th Edition). New York: McGraw-Hill Book Co., 1979

22. Pajayakrit, Palanut. "A Wind Tunnel Study of the Effects of Lower Surface Blowing on the Lift, Drag, and Lift-to-Drag Ratio of a Circulation Control Airfoil," Unpublished Master's Thesis, Wright-Patterson AFB, OH: Air Force Institute of Technology, July 1980.

APPENDIX A

Model Description/Experimental Setup and Proposed Trailing Edge Modification

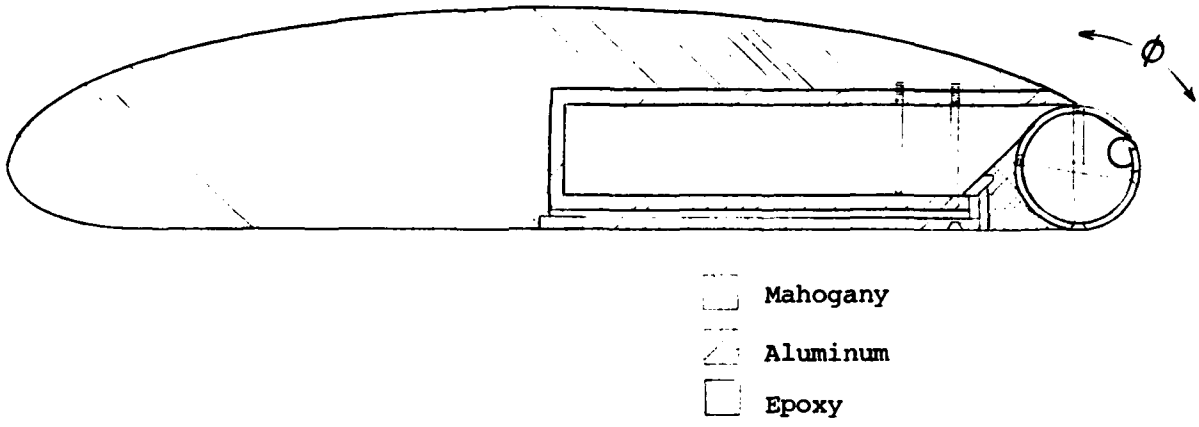

Figure A-1 Airfoil/Model Geometry

An algebraic description of the exterior surfaces of the airfoil is as follows:

Upper Surface

$$Y = .2874\sqrt{10^2-(10-X)^2} \qquad \text{for } 0 \leq X \leq 19.2 \text{ in}$$

Lower Surface

$$Y = -.55315\sqrt{2^2-(2-X)^2} \qquad \text{for } 0 \leq X \leq 2.0 \text{ in}$$

$$Y = -1.1263 \qquad \text{for } 2.0 \leq X \leq 19.2 \text{ in}$$

Cylindrical Surface

$$Y = -0.01 \pm \sqrt{(1.1163)^2 - (19.2-X)^2}$$

$$\text{for } 18.0837 \leq X \leq 20.3163 \text{ in}$$

The work of Pajayakrit (Ref 22) and Haupt (Ref 9) identified difficulties in obtaining good flow attachment after the blowing slot. These difficulties appear to have been caused by the following flow conditions; first, the flow exiting the plenum was not tangential to the downstream surface, and second, without the tangential flow the adverse pressure gradient is too severe for the flow to reattach. For these reasons, the plenum and Coanda surfaces of this model were designed first to insure that the flow would be tangent to the downstream surface at the slot exit plane and second to produce a local favorable pressure gradient just downstream of the slot improving the flow attachment conditions.

The aft section of the main plenum was molded out of epoxy to provide an accurate mating surface for the circular trailing edge. A spanwise slot was milled into the mating surface and a 0.032 in by twenty-six in piece of plastic tubing was used to improve the seal between the cylinder and the main plenum.

A second difficulty identified by Pajayakrit and Haupt was that of an uneven spanwise pressure distribution. To reduce this problem, two screens were placed spanwise inside the main plenum to distribute the mass flow in a more uniform fashion (Fig. A-2). In addition, a three dimensional foam insert was placed just in front of the second screen to act as a flow straightener. When these screens and straighteners were used the model exhibited a uniform spanwise pressure distribution within a few percent and no noticeable spanwise flow.

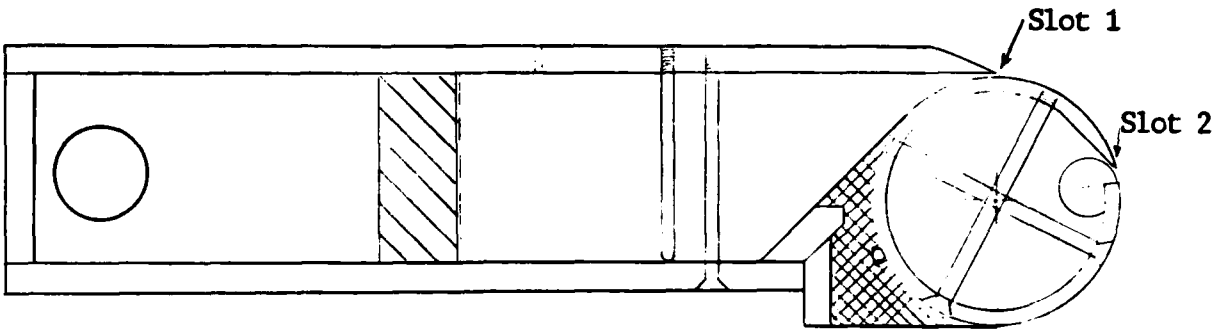

A. Section View

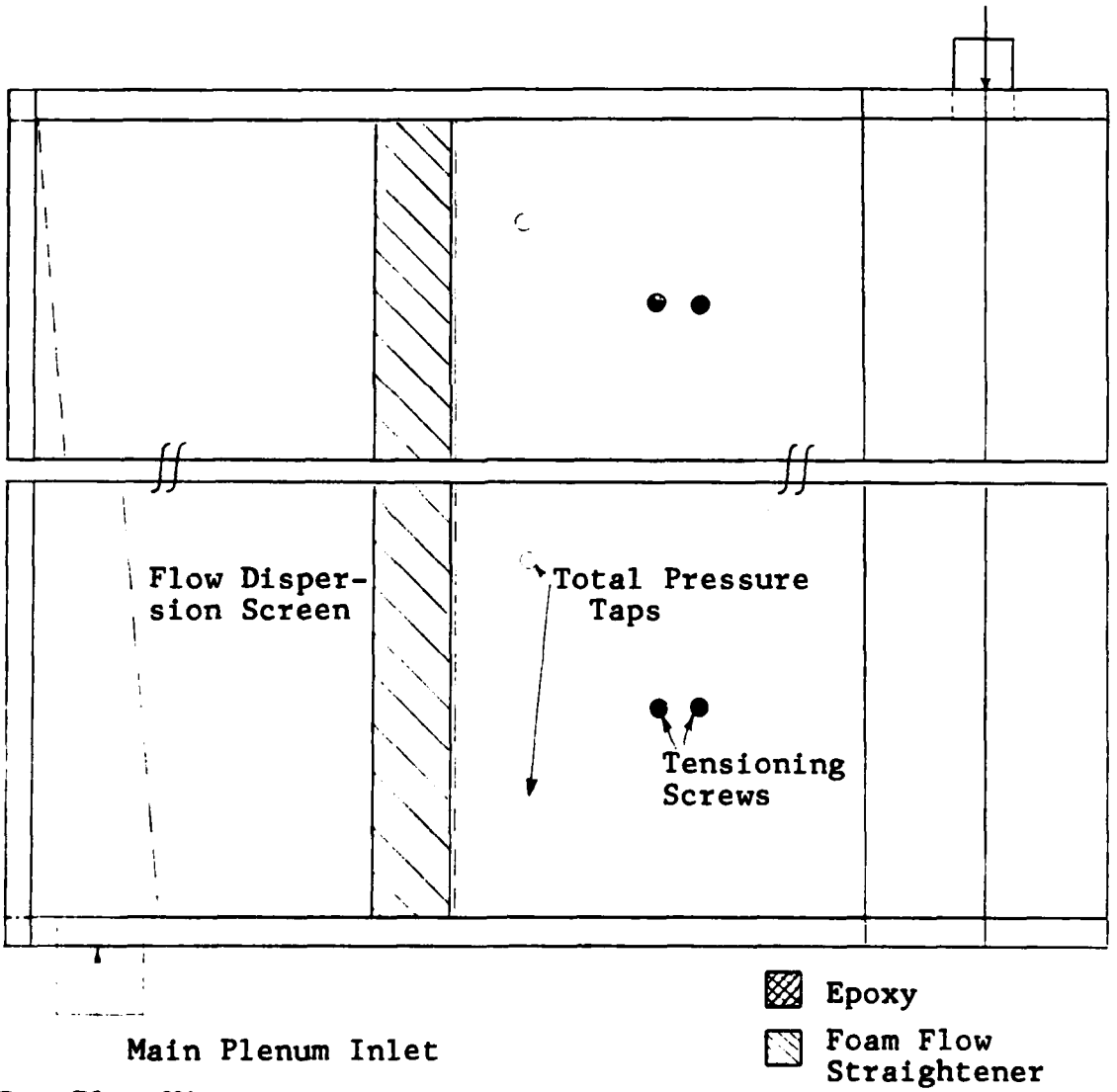

B. Plan View

Figure A-2 Main and Cylindrical Plenum Design

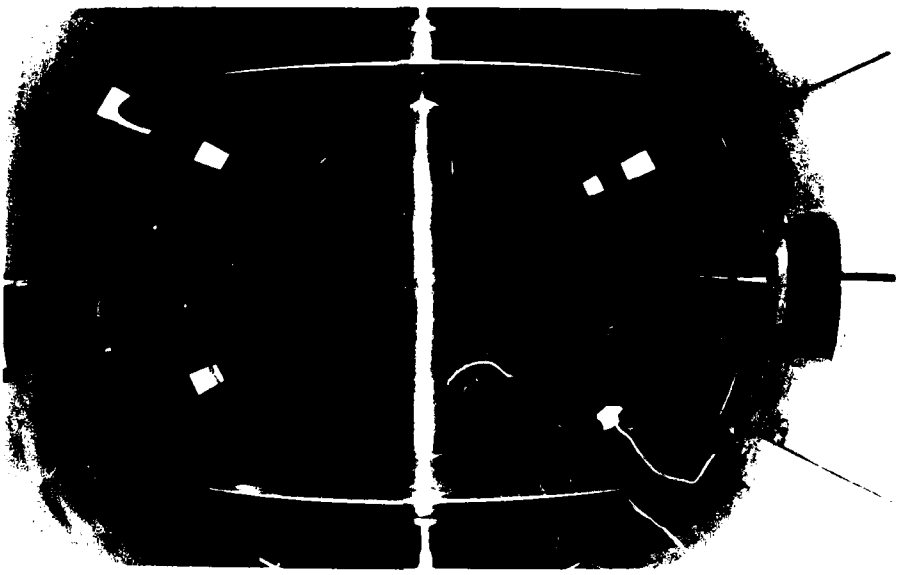

FIG A-3 A leading edge view of the model in the test section with the wake survey rake in the background.

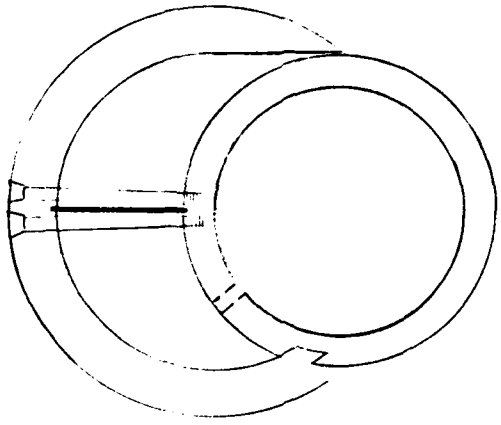

Figure A-4 Proposed Airfoil Modification to Enable Increased Dual Slot Performance

Although the results of the testing of this airfoil and trailing edge geometry reflect substantial improvements over the single slot configuration, the following modification is provided in an effort to improve the performance of the present design (Fig. A-4). Inefficiencies in the test item include three specific problems.

The use of the small radius rod for the original cylindrical plenum Coanda surface introduced the following two problems:

1. The blowing air introduced at this slot was required to turn through 36 deg before it could directly affect the external flow field. Therefore, the velocity in the boundary layer of the jet is reduced somewhat before the jet effects changes in the external flow field. This

reduction in the boundary layer velocity leads to earlier jet separation and reduced lift augmentation capability.

2. After turning the initial 36 deg of rotation, the Coanda surface transitions from the 0.5 in diameter rod to the 1.116 in diameter cylindrical surface (Fig A-1 and A-2). This by itself is not a problem; however, any failure to exactly match the two surfaces at their junction can lead to premature jet separation.

Due to the method of introducing the secondary air into the cylindrical plenum and the use of cross bar stiffeners, the flow in this plenum was not entirely uniform and introduces some three-dimensional effects though they were small.

The trailing edge modification removes these problems in the following ways:

1. Using the larger radius cylinder in the place of the 0.5 in diameter rod and translating the centerline, enables the jet to effect changes in the exterior flow field immediately after exiting the slot. This enables the jet to effect maximum changes to the exterior flow field.

2. By using the larger radius cylinder, the transition point between the internal cylinder and the external cylinder has been rotated from 36 deg to 180 deg. Therefore any interface errors introduced by machining difficulties should not cause premature jet separation.

3. By introducing the secondary air supply into the center of the interior cylinder and introducing a flow

straightening foam insert and screen, the flow should be much more uniform spanwise. Additionally, the thicker walled cylinders enable the placement of all the pressure tap lines in the cylinder walls thereby reducing any interference with the secondary air leading up to the slot exit plane.

TABLE A-1

Pressure Tap Locations Two-Dimensional Model

Pressure Tap Locations

Upper		Lower		Cylinder	
Tap No.	X/c	Tap No.	X/c	Tap No.	θ Deg
U/L 1	0.0	U/L 1	0.0	C1	0
U2	0.0049	L2	0.0049	C2	20
U3	0.0098	L3	0.0098	C3	40
U4	0.0148	L4	0.0148	C4	60
U5	0.0197	L5	0.0197	C5	80
U6	0.0246	L6	0.0246	C6	90
U7	0.0295	L7	0.0295	C7	100
U8	0.0344	L8	0.0344	C8	120
U9	0.0394	L9	0.0394	C9	140
U10	0.0443	L10	0.0443	C10	180
U11	0.0492	L11	0.0492	C11	200
U12	0.0984	L12	0.0738	C12	220
U13	0.1477	L13	0.0984	C13	240
U14	0.1969	L14	0.1477	C14	260
U15	0.2461	L15	0.1969	C15	280
U16	0.2953	L16	0.2461	C16	300
U17	0.3446	L17	0.2953	C17	320
U18	0.4430	L18	0.3446	C18	0
U19	0.4971	L19	0.4430	C19	90
U20	0.5414	L20	0.5168	C20	180
U21	0.6399	L21	0.6891	C21	0
U22	0.6891	L22	0.8860	C22	90
U23	0.7383	L23	0.9204	C23	180
U24	0.8368				
U25	0.8860				
U26	0.9104				
U27	0.9352				

The angle θ is fixed to the cylinder and increments in the clockwise direction, with $\theta = 0$, one hundred eighty degrees from the junction of the .5 in diameter rod and the external cylinder.

APPENDIX B

Graphical Information

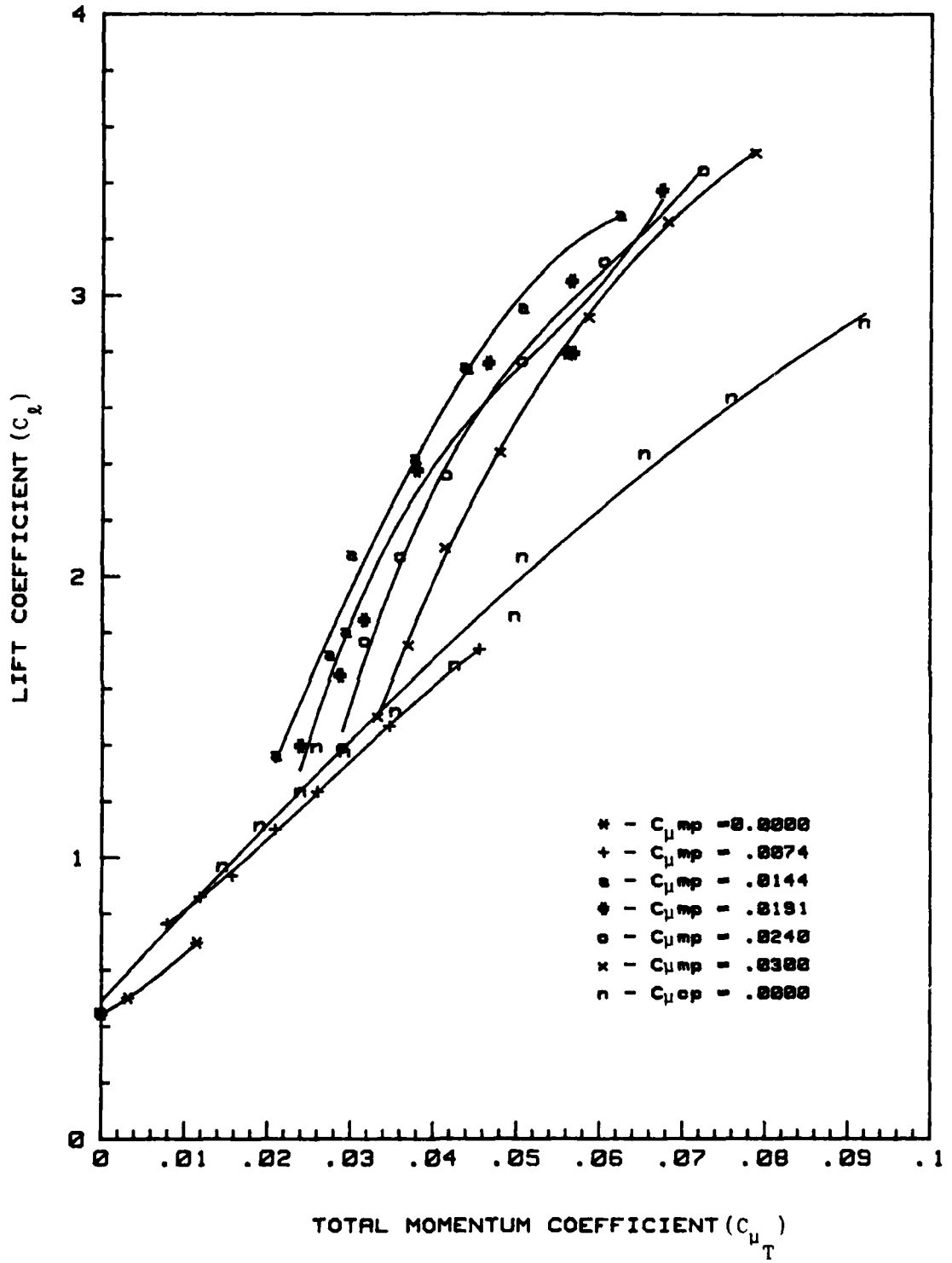

FIG B-1 LIFT AS A FUNCTION OF TOTAL MOMENTUM COEFFICIENT ($\emptyset$ =73.5) FOR CURVES OF CONSTANT MAIN PLENUM MOMENTUM COEFFICIENT

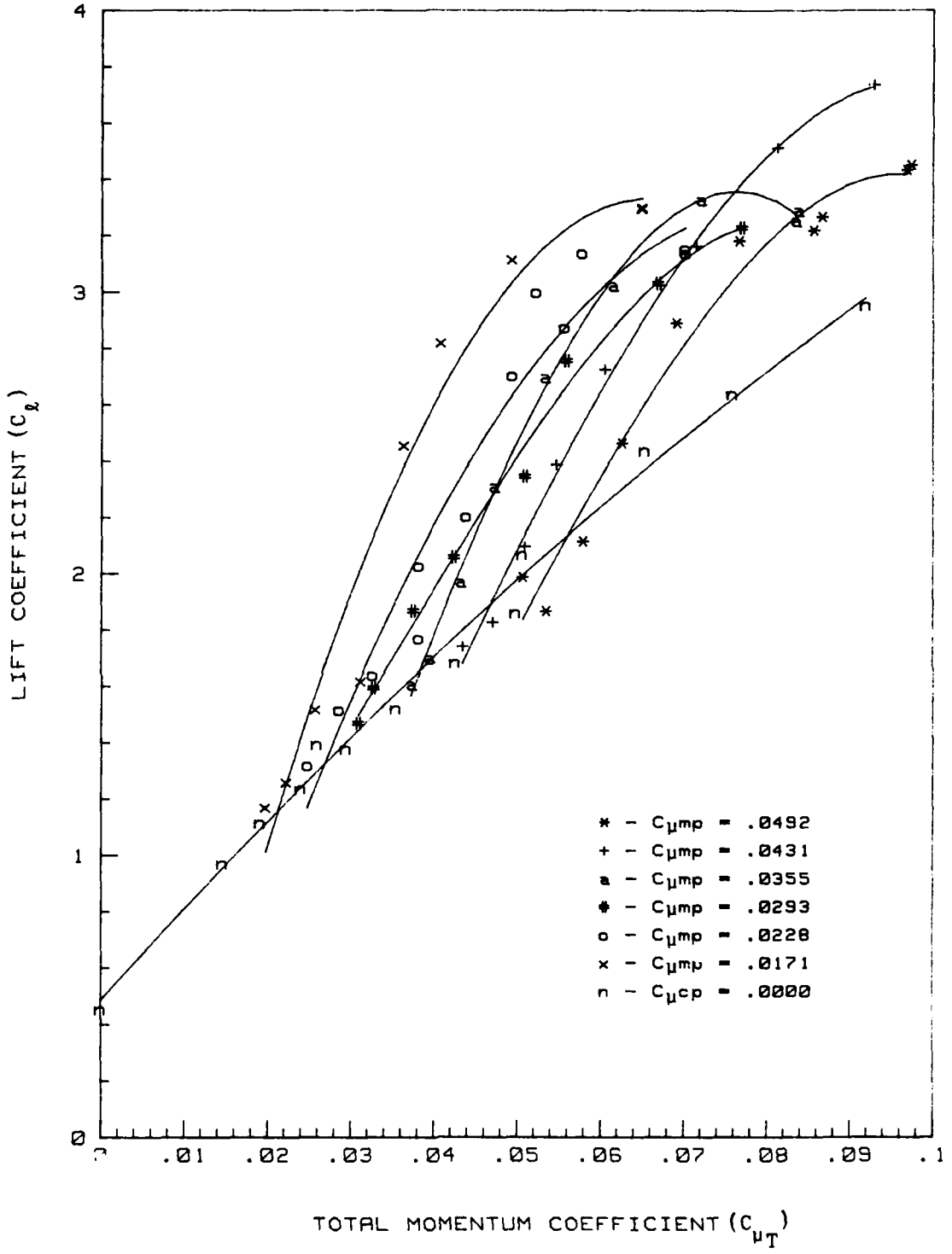

FIG B-2 LIFT AS A FUNCTION OF TOTAL MOMENTUM COEFFICIENT ($\emptyset$ =83.5) FOR CURVES OF CONSTANT MAIN PLENUM MOMENTUM COEFFICIENT

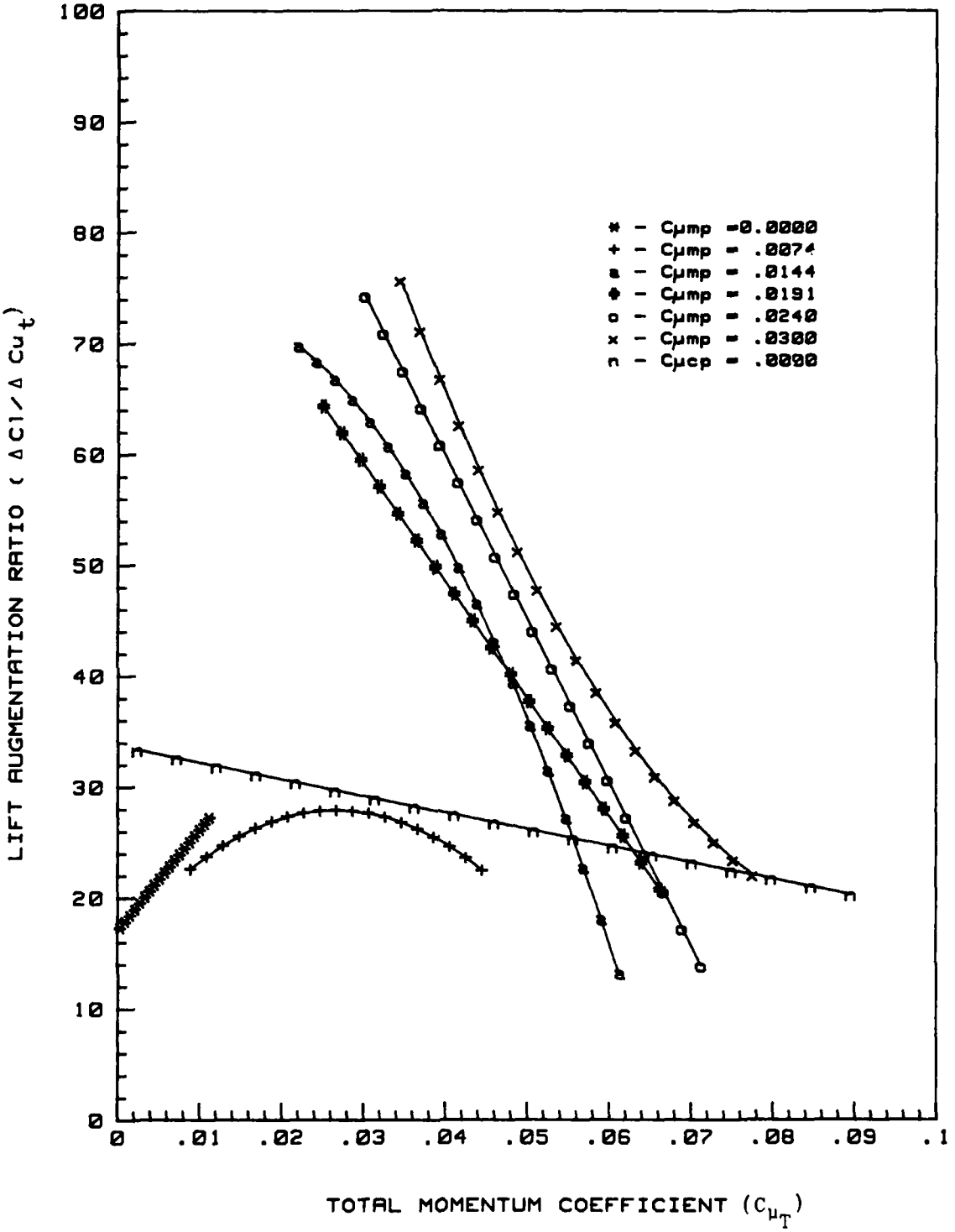

FIG B-3 LIFT AUGMENTATION VERSUS TOTAL MOMENTUM COEFFICIENT (Ø =73.5)
FOR CURVES OF CONSTANT MAIN PLENUM MOMENTUM COEFFICIENT

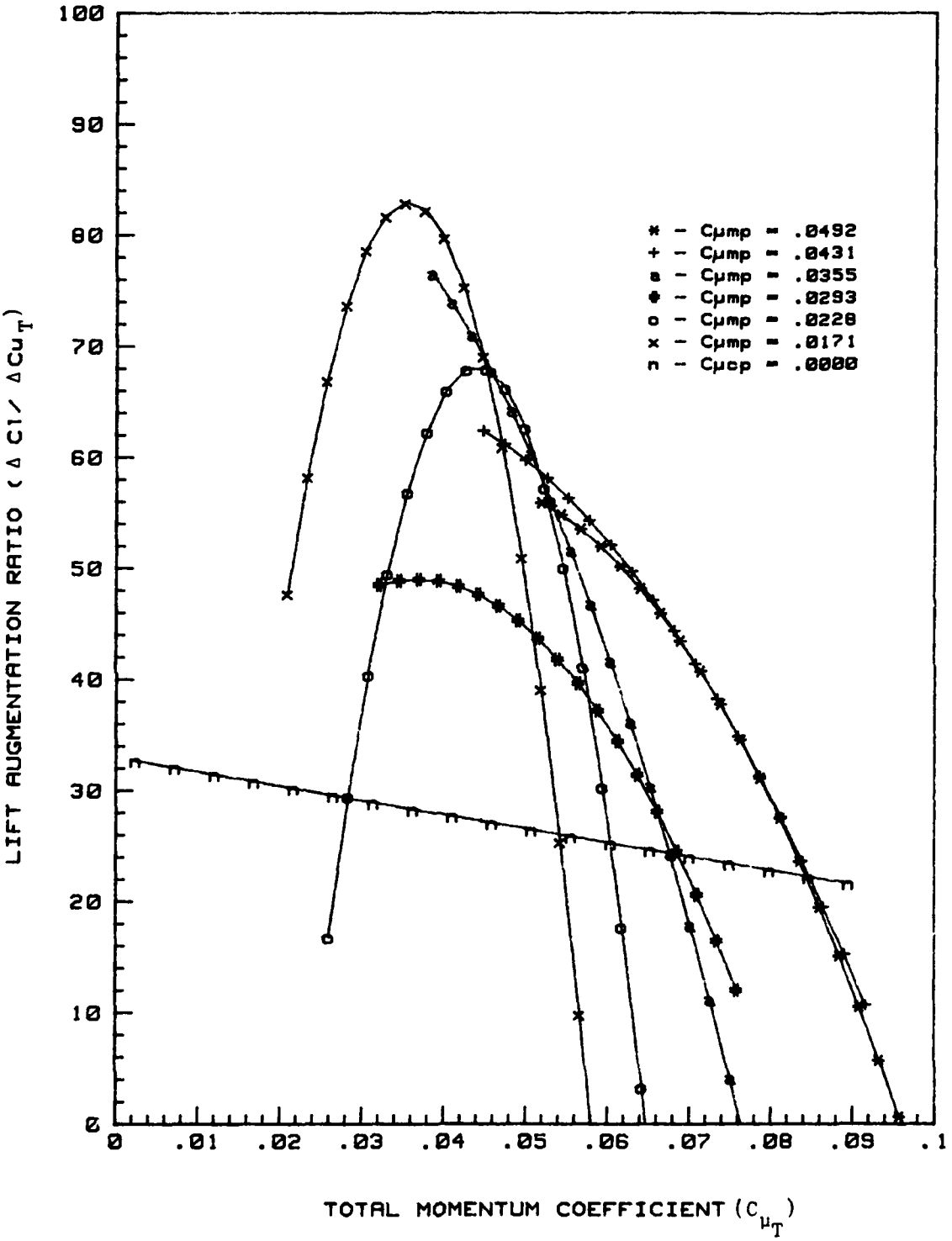

FIG B-4 LIFT AUGMENTATION VERSUS TOTAL MOMENTUM COEFFICIENT (Ø =83.5)
FOR CURVES OF CONSTANT MAIN PLENUM MOMENTUM COEFFICIENT

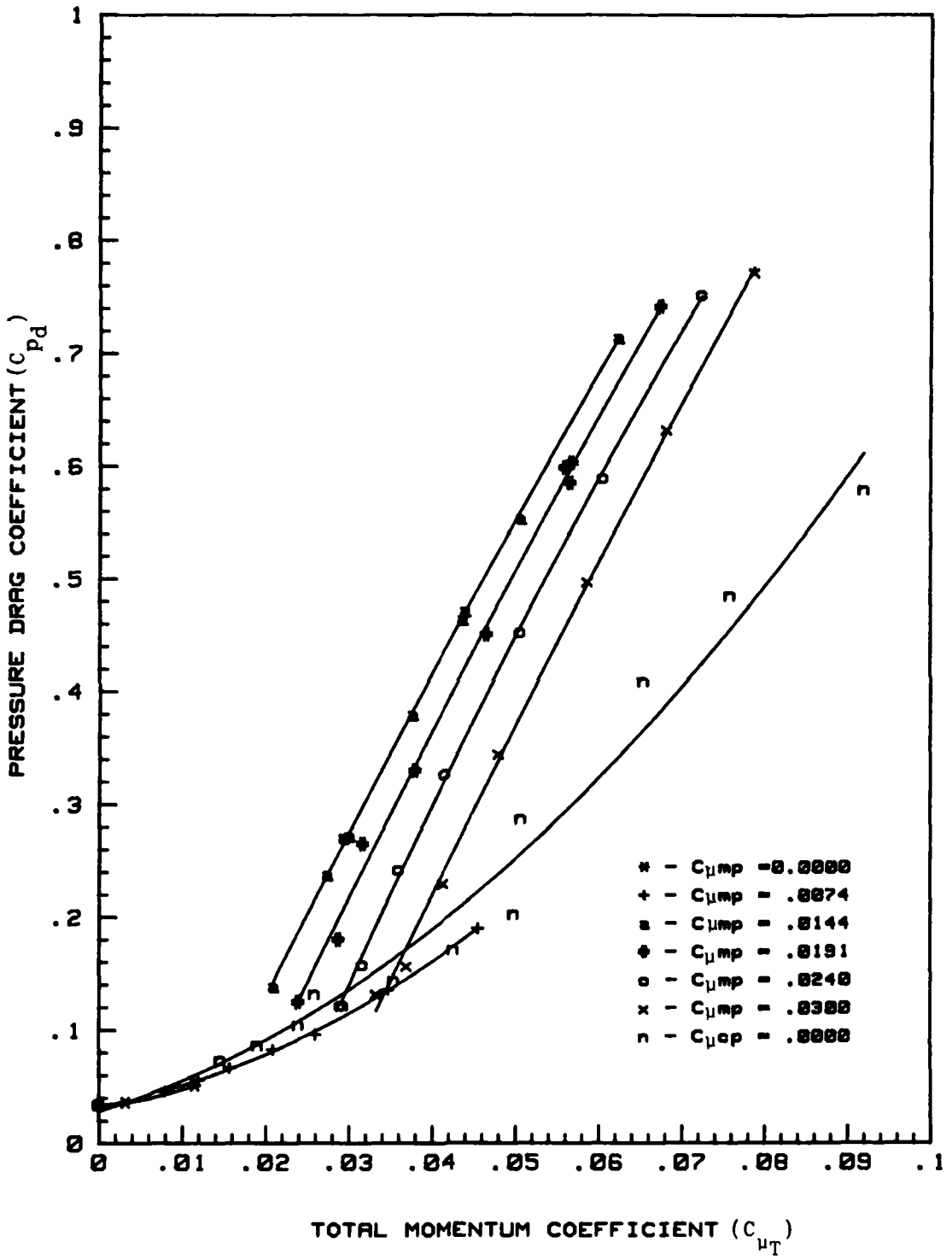

FIG B-5 PRESSURE DRAG VERSUS TOTAL MOMENTUM COEFFICIENT (ϕ =73.5) FOR CURVES OF CONSTANT MAIN PLENUM MOMENTUM COEFFICIENT

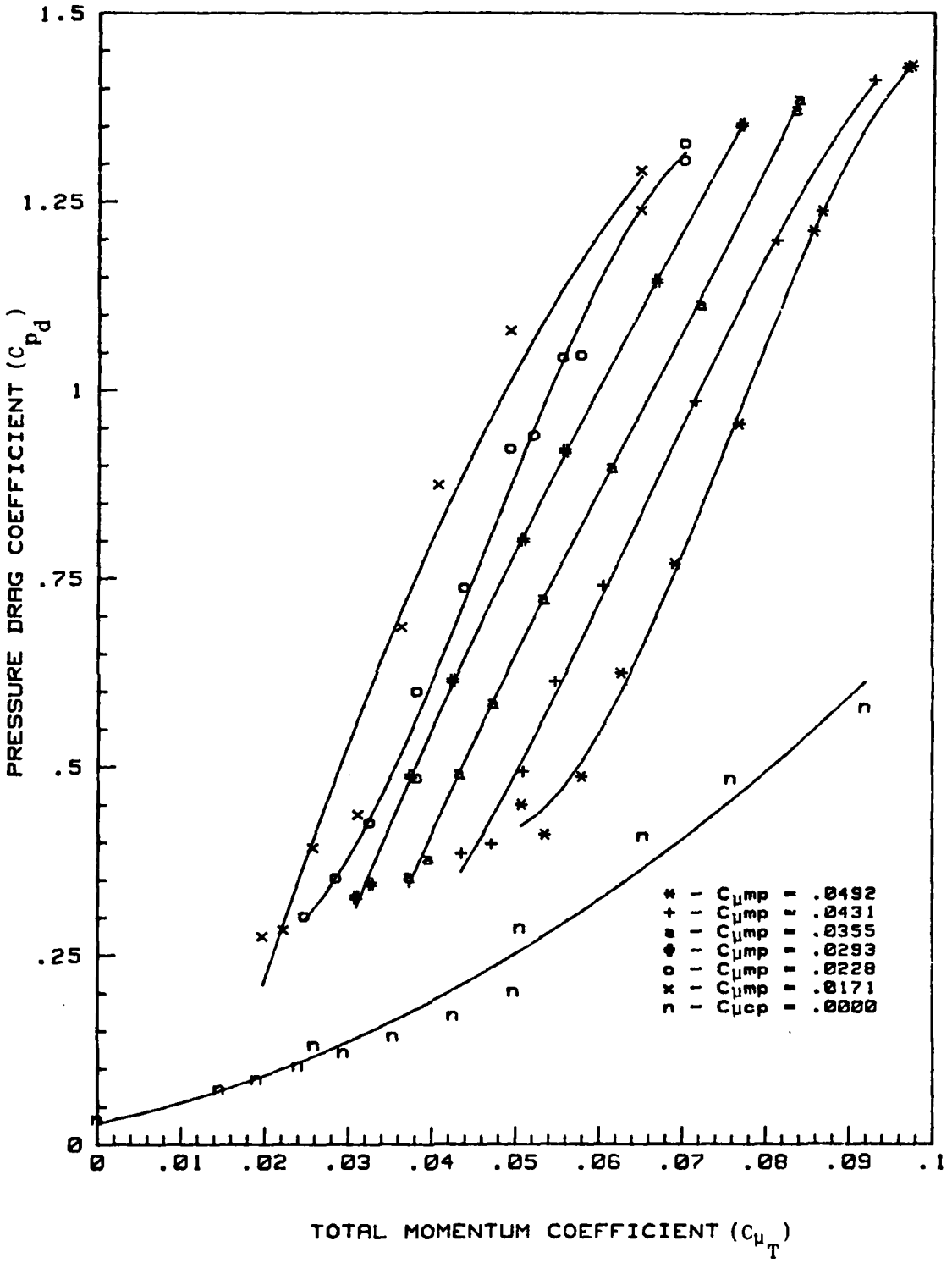

FIG B-6 PRESSURE DRAG VERSUS TOTAL MOMENTUM COEFFICIENT (Ø=83.5) FOR CURVES OF CONSTANT MAIN PLENUM MOMENTUM COEFFICIENT

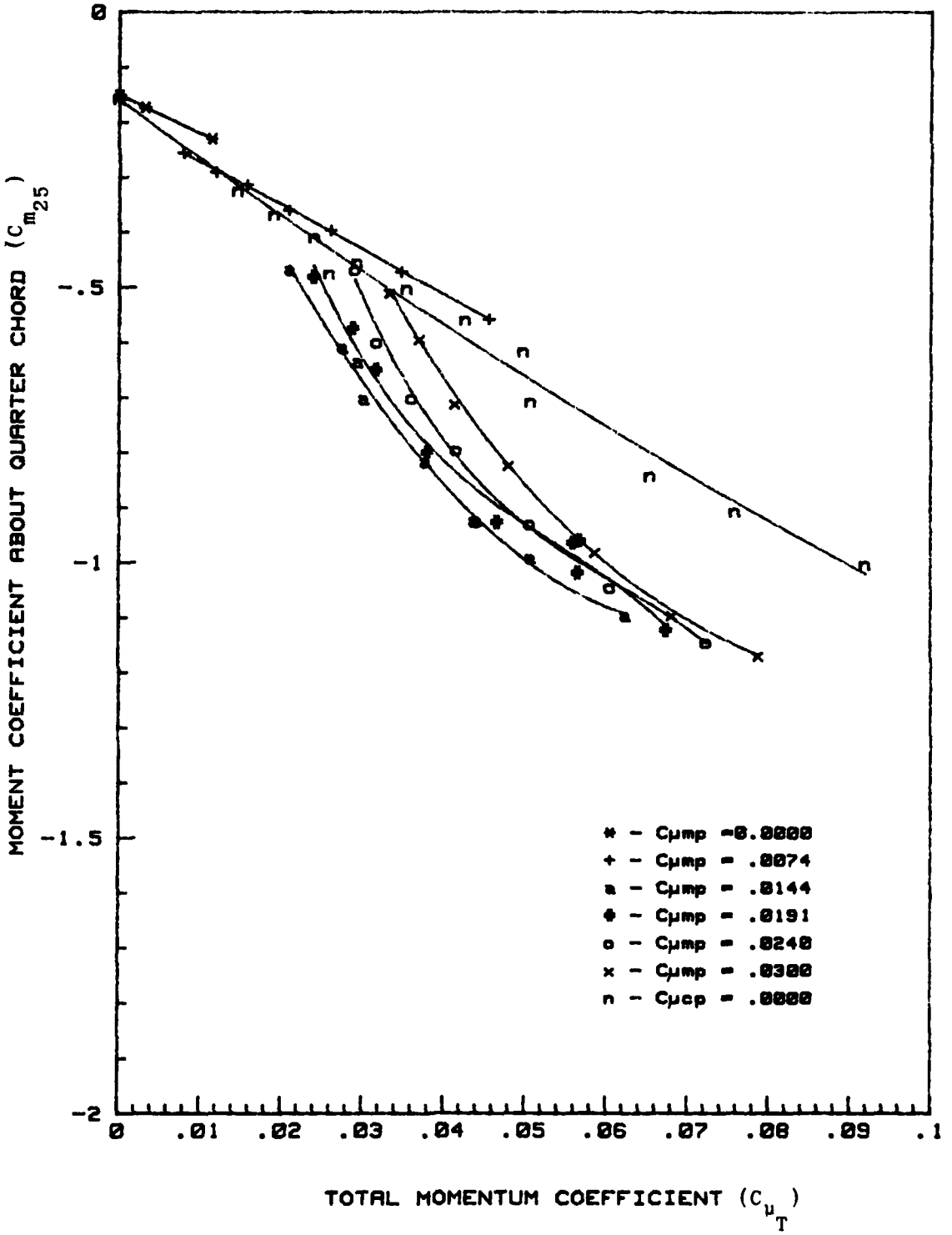

FIG B-7 MOMENT AS A FUNCTION OF TOTAL MOMENTUM COEFFICIENT (Ø=73.5) FOR CURVES OF CONSTANT MAIN PLENUM MOMENTUM COEFFICIENT

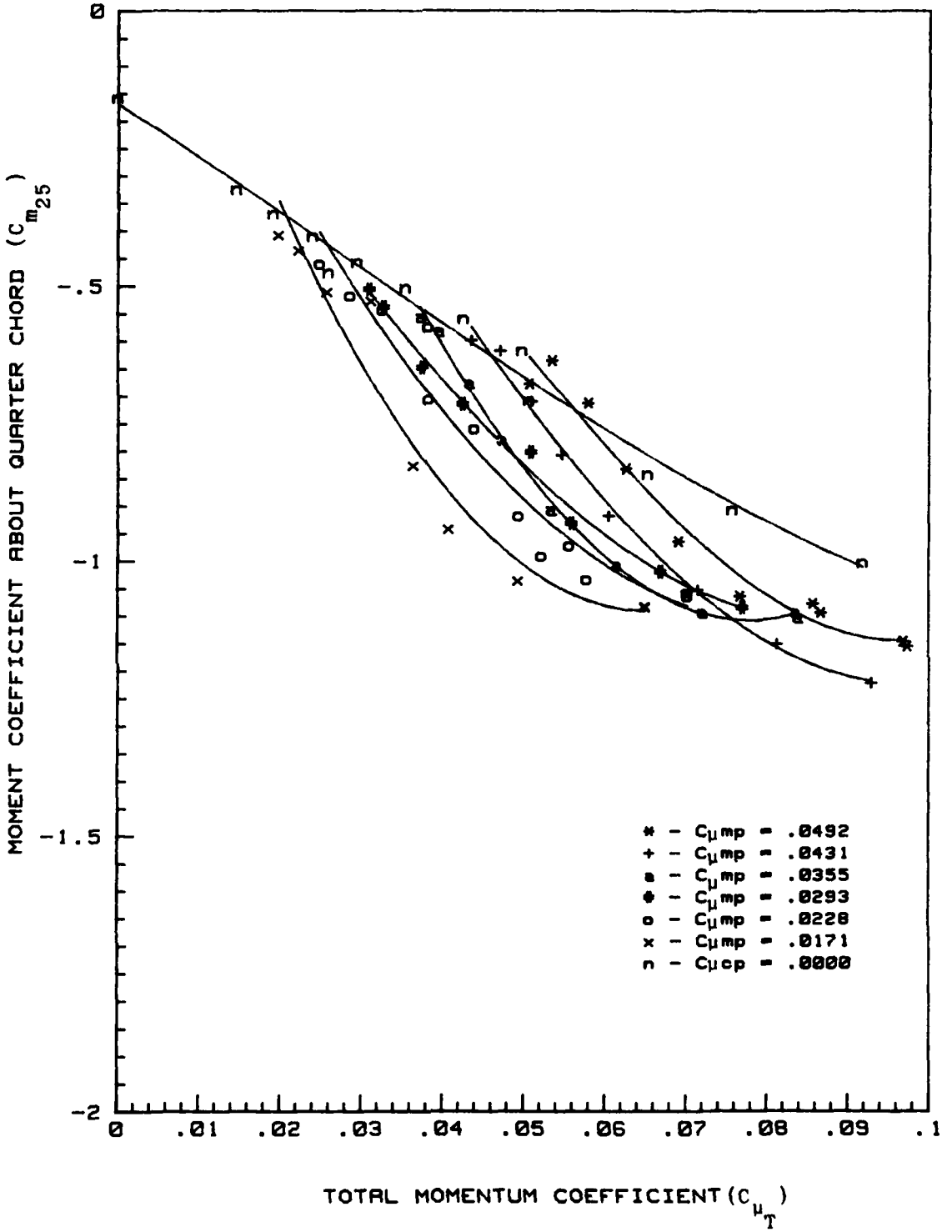

FIG B-8 MOMENT AS A FUNCTION OF TOTAL MOMENTUM COEFFICIENT ($\emptyset$ =83.5) FOR CURVES OF CONSTANT MAIN PLENUM MOMENTUM COEFFICIENT

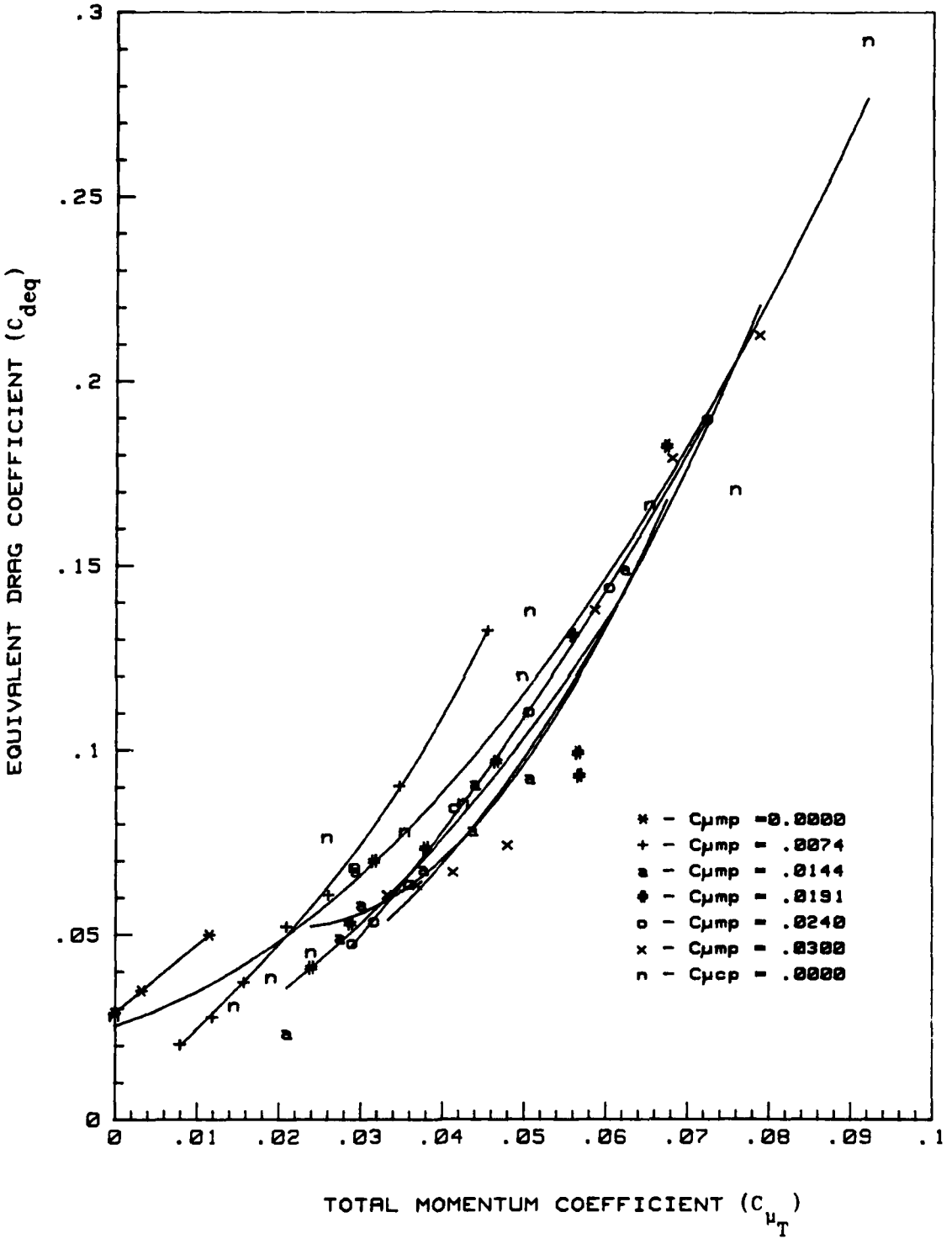

FIG B-9 DRAG AS A FUNCTION OF TOTAL MOMENTUM COEFFICIENT ($\emptyset$ =73.5) FOR CURVES OF CONSTANT MAIN PLENUM MOMENTUM COEFFICIENT

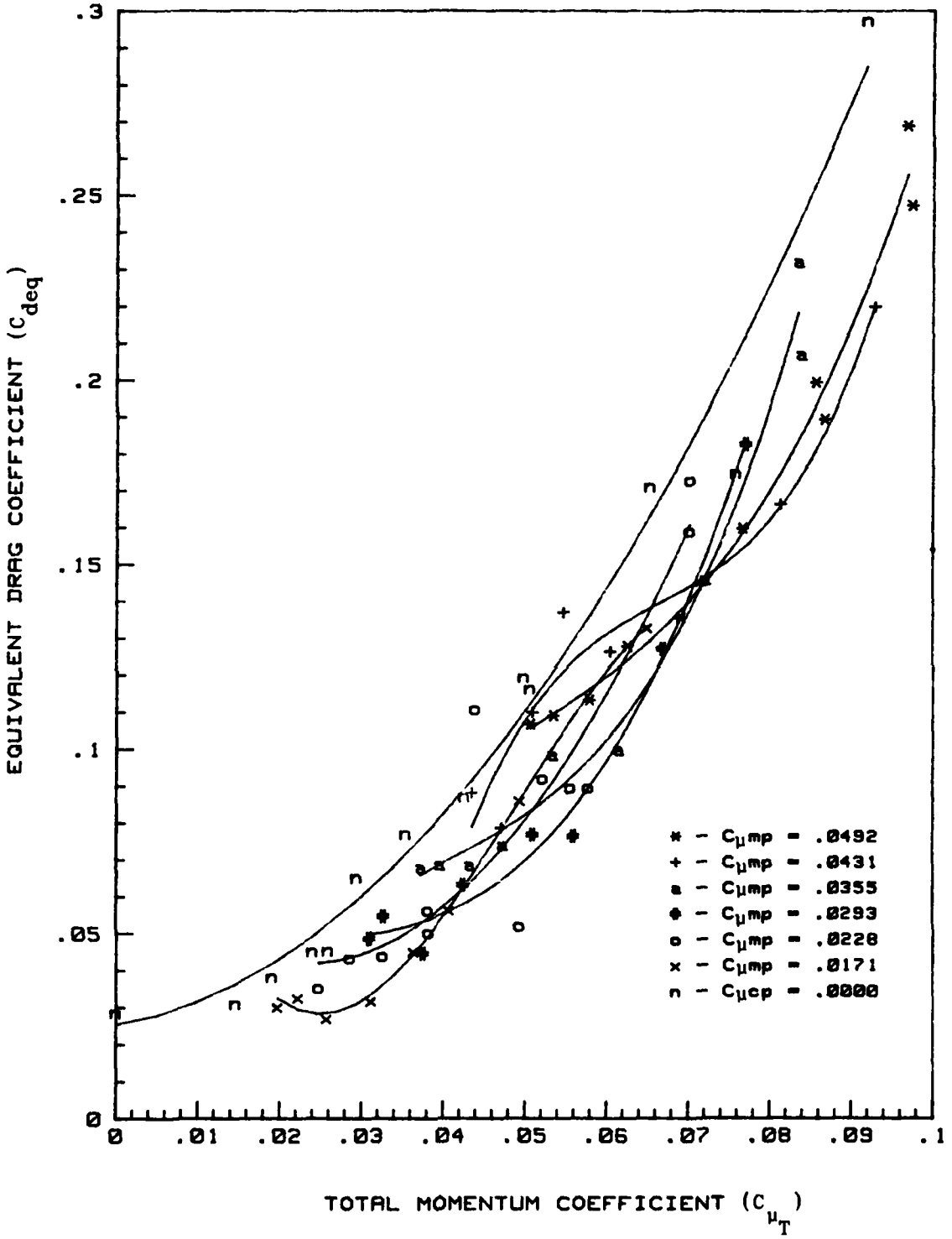

FIG B-10 DRAG AS A FUNCTION OF TOTAL MOMENTUM COEFFICIENT (ϕ =83.5) FOR CURVES OF CONSTANT MAIN PLENUM MOMENTUM COEFFICIENT

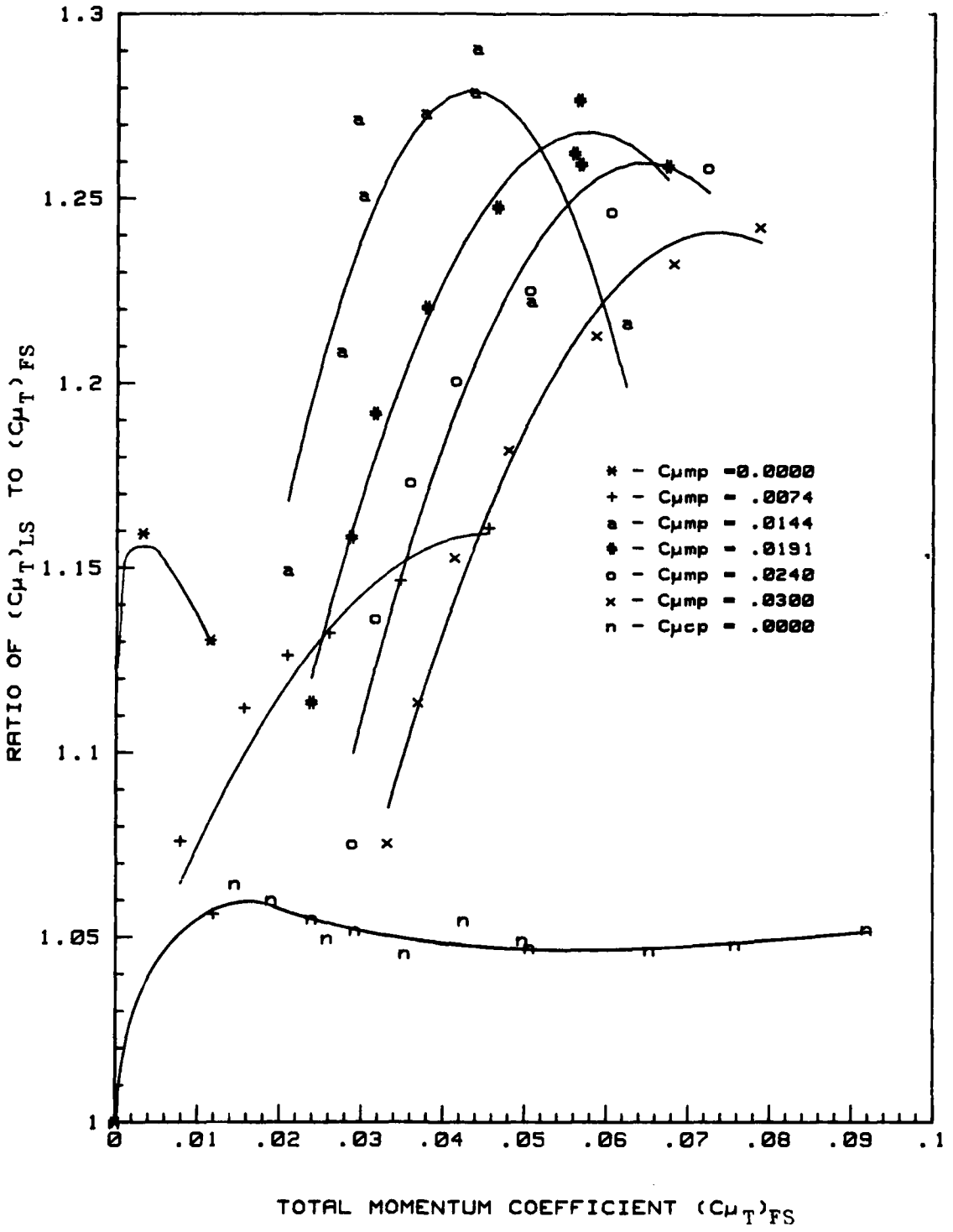

FIG B-11 RATIO OF $(C\mu_T)_{LS}$ TO $(C\mu_T)_{FS}$ VERSUS $(C\mu_T)_{FS}$ ($\emptyset$ =73.5) FOR CURVES OF CONSTANT MAIN PLENUM MOMENTUM COEFFICIENT

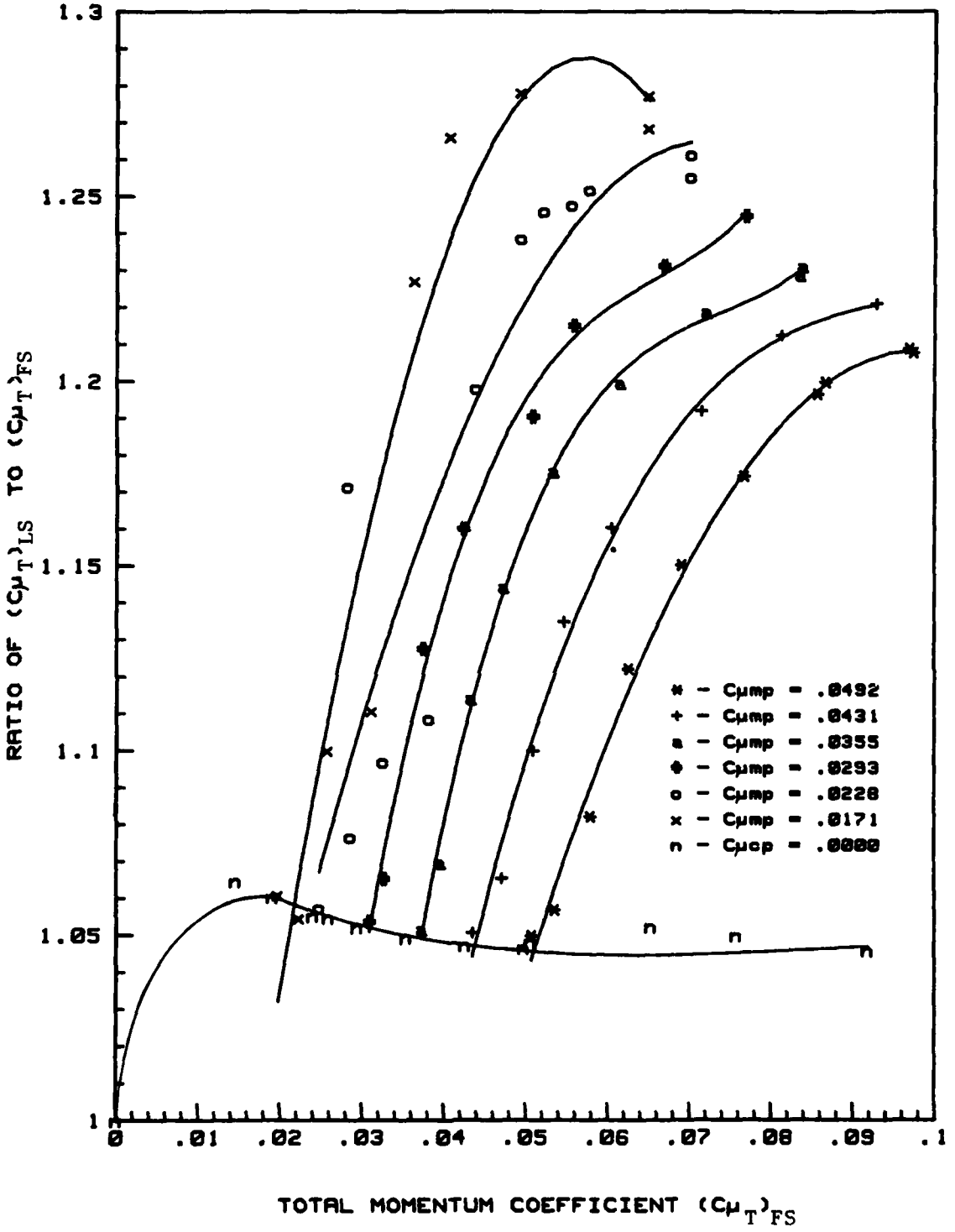

FIG B-12 RATIO OF $(C\mu_T)_{LS}$ TO $(C\mu_T)_{FS}$ VERSUS $(C\mu_T)_{FS}$ ($\emptyset$ =83.5) FOR CURVES OF CONSTANT MAIN PLENUM MOMENTUM COEFFICIENT

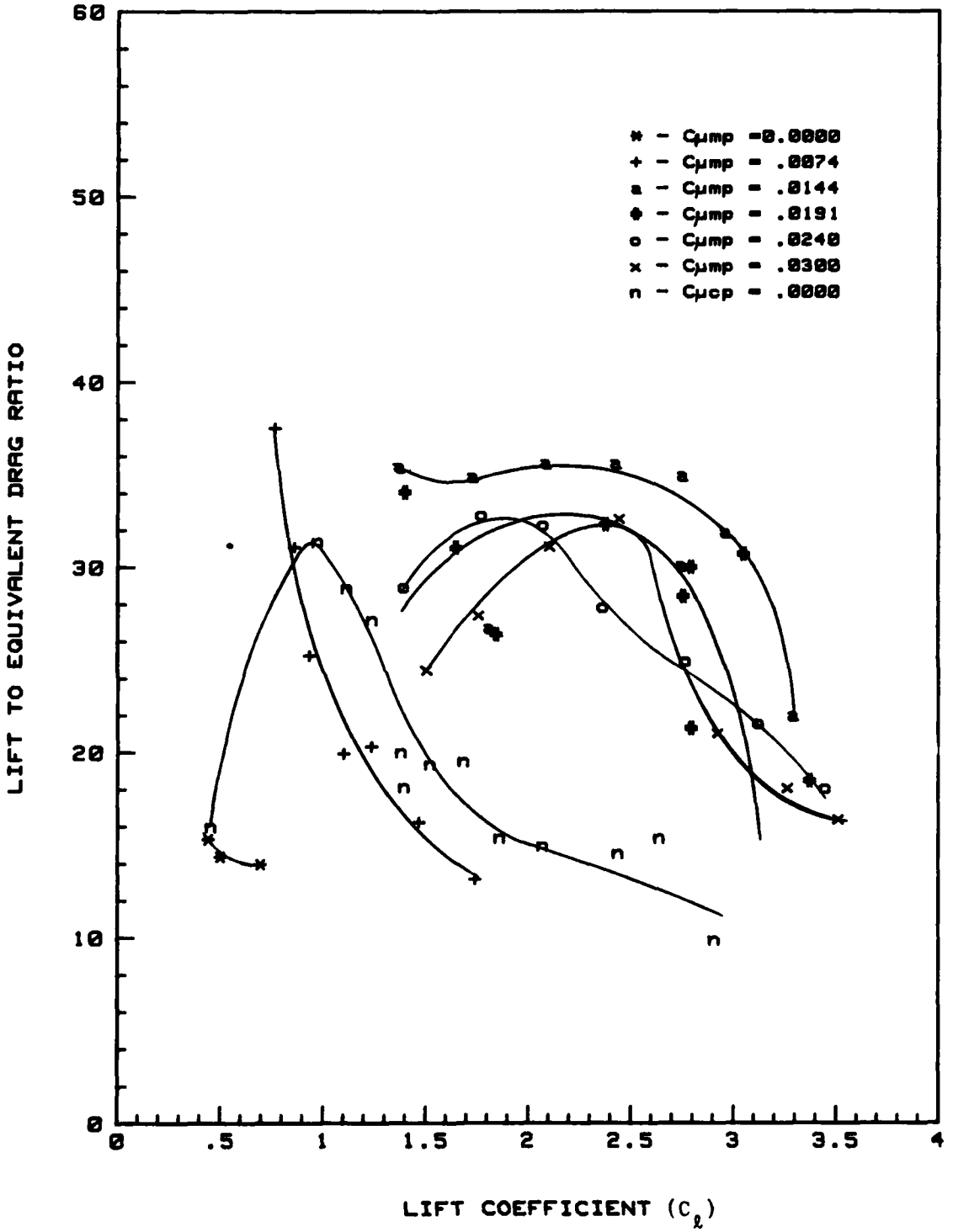

FIG B-13 LIFT TO EQUIVALENT DRAG RATIO AS A FUNCTION OF LIFT (ϕ =73.5) FOR CURVES OF CONSTANT MAIN PLENUM MOMENTUM COEFFICIENT

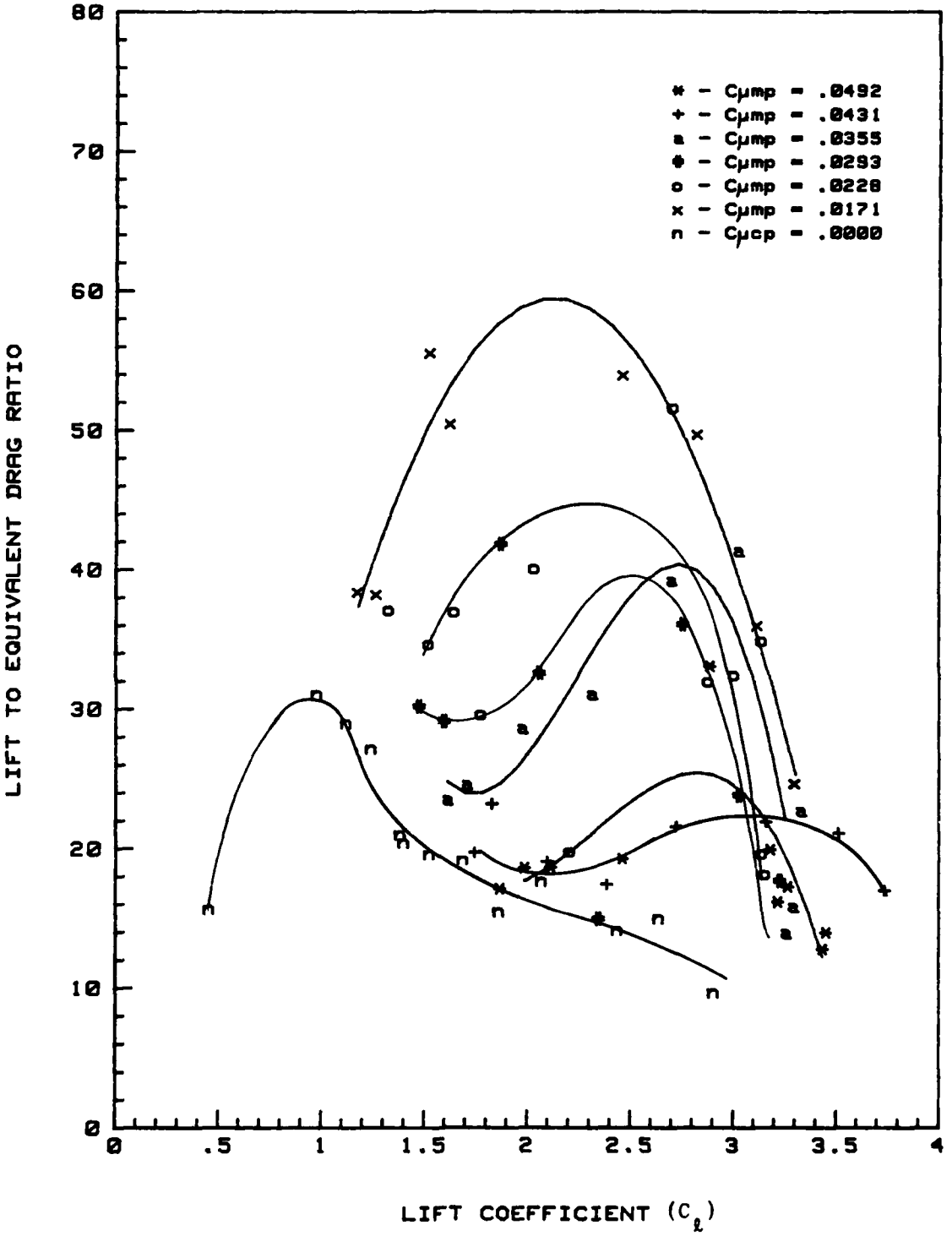

FIG B-14 LIFT TO EQUIVALENT DRAG RATIO AS A FUNCTION OF LIFT ($\emptyset$ =83.5) FOR CURVES OF CONSTANT MAIN PLENUM MOMENTUM COEFFICIENT

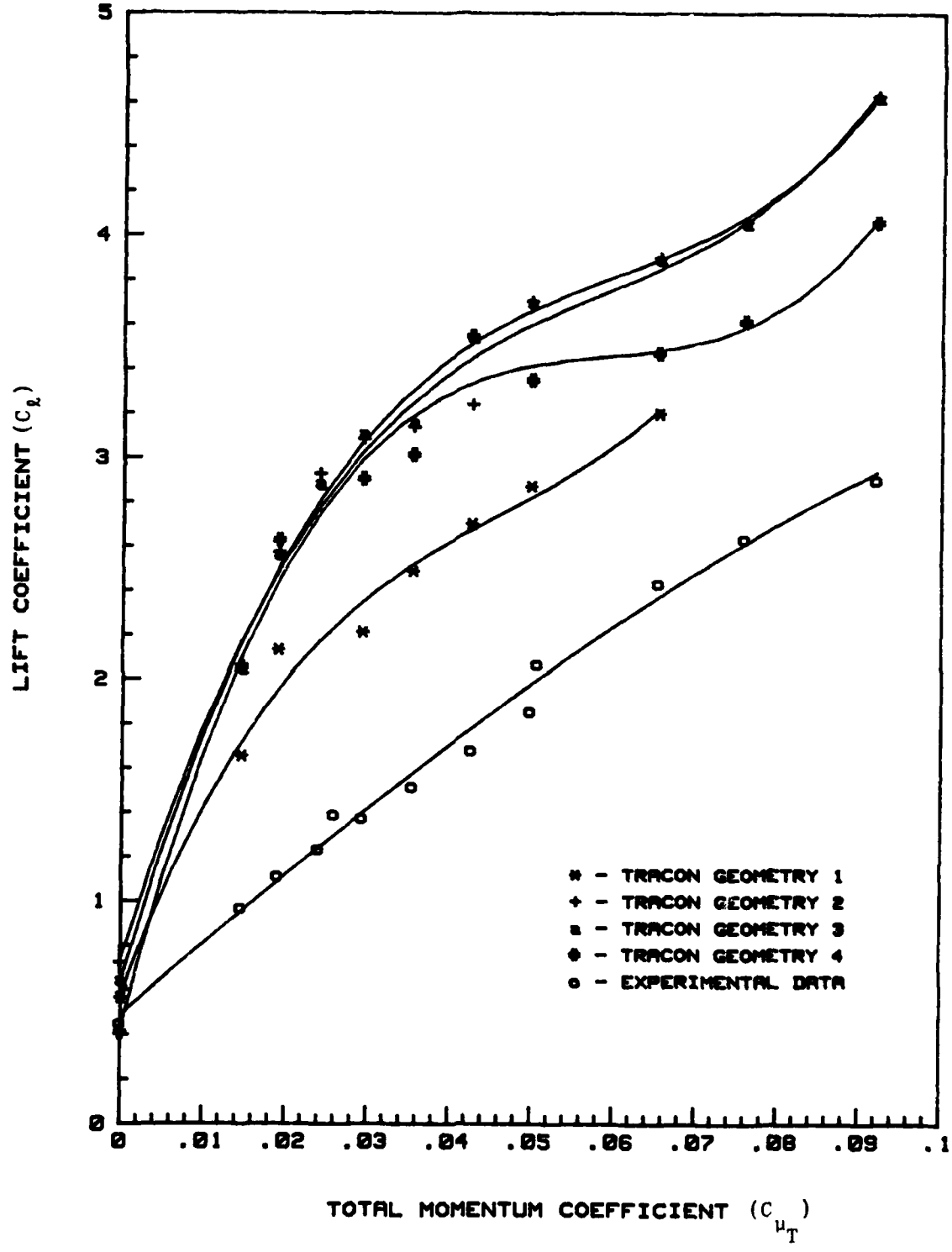

FIG B-15 COMPARISON OF LIFT RESULTS PREDICTED BY TRACON WITH BASELINE EXPERIMENTAL DATA

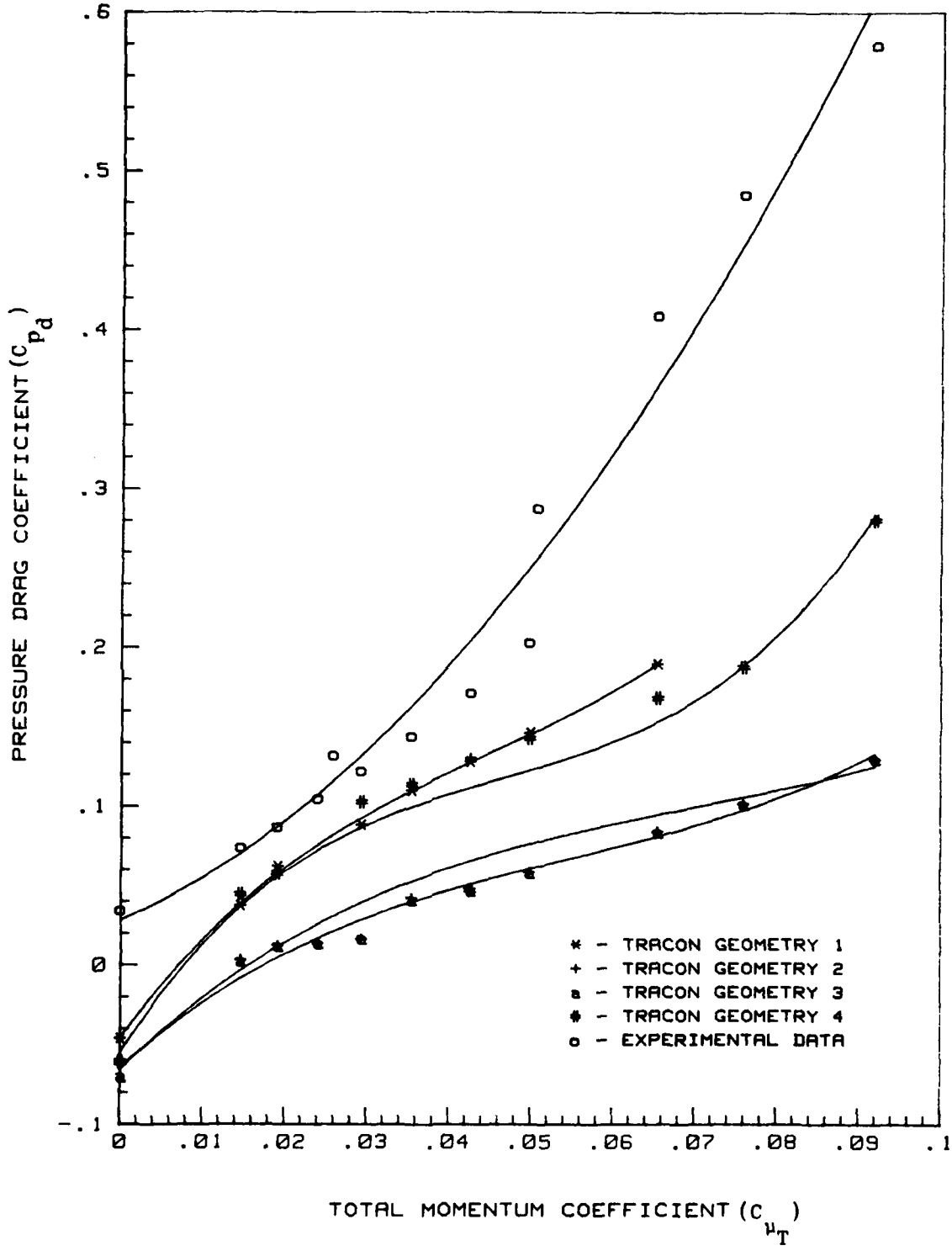

FIG B-16 COMPARISON OF PRESSURE DRAG RESULTS PREDICTED BY TRACON WITH BASELINE EXPERIMENTAL DATA

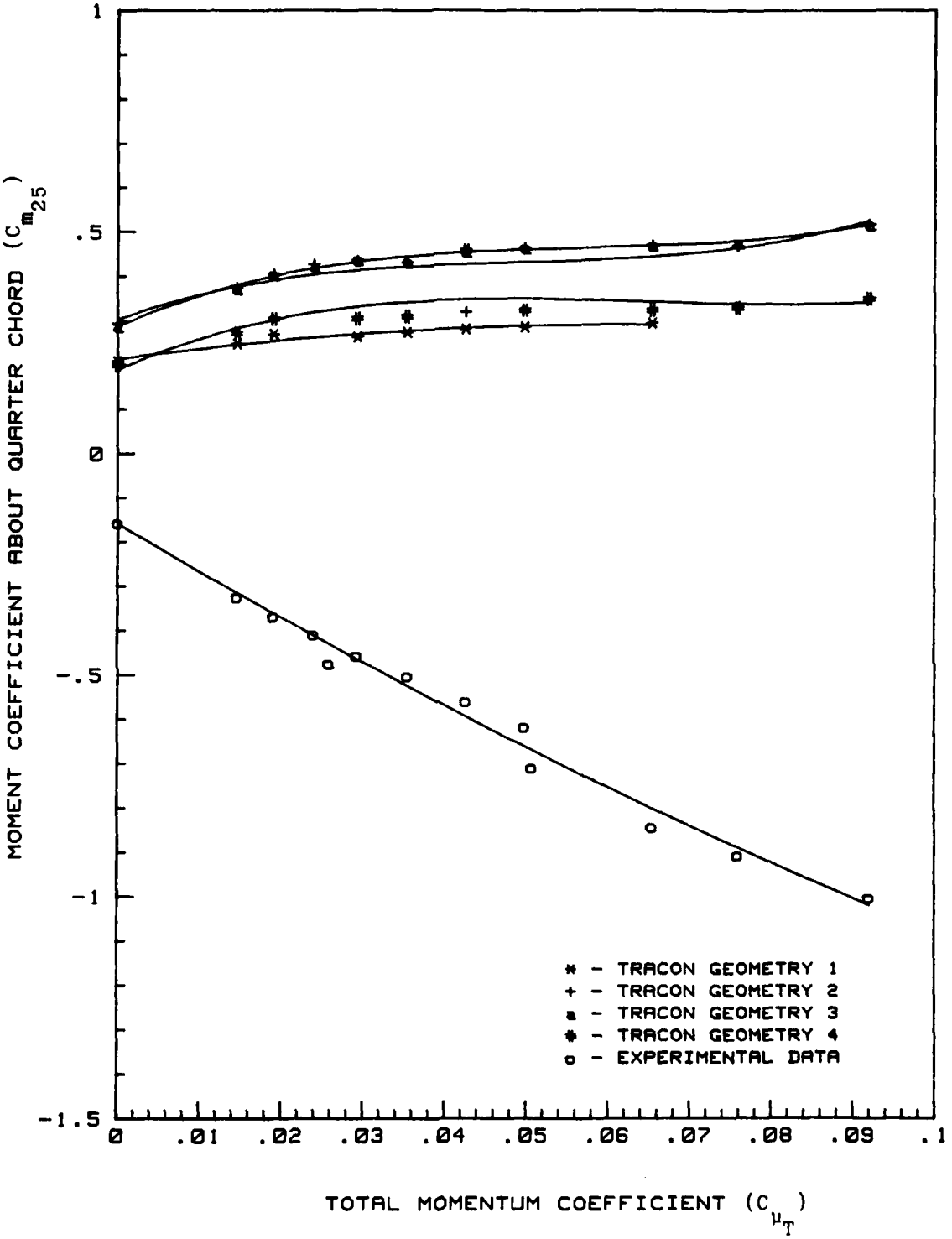

FIG B-17 COMPARISON OF MOMENT RESULTS PREDICTED BY TRACON WITH BASELINE EXPERIMENTAL DATA

Vita

John K. Harvell was born 20 August 1956 in Madison, Wisconsin. In 1974 he graduated from Merrimack High School in Merrimack, New Hampshire. In May of 1978 he received a Bachelor of Science degree (Mechanical Engineering) from Norwich University in Northfield, Vermont. Upon graduation, he attended the USAF Summercamp at Rickenbacker AFB where upon completion he was commissioned a 2d Lieutenant in the USAF. He was called to active duty in November 1978. He worked as a research and development munitions test engineer for the Terminal Effects Branch, Munition Test Division, of the 3246th Test Wing at Eglin AFB, Florida until May 1981, when he entered the School of Engineering, Air Force Institute of Technology.

Permanent address: 8 Depot Street
Merrimack, New Hampshire 03054

SECURITY CLASSIFICATION OF THIS PAGE *(When Data Entered)*

REPORT DOCUMENTATION PAGE		READ INSTRUCTIONS BEFORE COMPLETING FORM
1. REPORT NUMBER AFIT/GAE/AA/82D-13	2. GOVT ACCESSION NO. A124732	3. RECIPIENT'S CATALOG NUMBER
4. TITLE *(and Subtitle)* An Experimental/Analytical Investigation Into the Performance of a 20-Percent Thick, 8.5-Percent Cambered, Circulation Controlled Airfoil		5. TYPE OF REPORT & PERIOD COVERED MS Thesis 6 PERFORMING ORG. REPORT NUMBER
7. AUTHOR(s)		8. CONTRACT OR GRANT NUMBER(s)
9. PERFORMING ORGANIZATION NAME AND ADDRESS Air Force Institute of Technology (AFIT-EN) Wright Patterson AFB Ohio 45433		10. PROGRAM ELEMENT, PROJECT, TASK AREA & WORK UNIT NUMBERS
11. CONTROLLING OFFICE NAME AND ADDRESS		12. REPORT DATE Dec 1982 13. NUMBER OF PAGES 69
14. MONITORING AGENCY NAME & ADDRESS*(if different from Controlling Office)*		15. SECURITY CLASS. *(of this report)* UNCLASSIFIED 15a. DECLASSIFICATION/DOWNGRADING SCHEDULE

16. DISTRIBUTION STATEMENT *(of this Report)*

Approved for public release; distribution unlimited

17. DISTRIBUTION STATEMENT *(of the abstract entered in Block 20, if different from Report)*

18. SUPPLEMENTARY NOTES

Approved for public release: IAW AFR 190-17.

LYNN E. WOLAVER
Dean for Research and Professional Development
Air Force Institute of Technology
Wright-Patterson AFB OH 45433

19 KEY WORDS *(Continue on reverse side if necessary and identify by block number)*

Circulation Control
Airfoil Test
Dual Slot
TRACON

20. ABSTRACT *(Continue on reverse side if necessary and identify by block number)*

This study was conducted to investigate the effect of two tangentially blown slots on the performance of a 20-percent thick, 8.5-percent cambered elliptical airfoil. Lift, drag, and moment coefficients were obtained at a test Reynolds number of 9.5×10^5 for secondary slot locations of 73.5 and 83.5 deg. Results show that the use of two tangentially blown slots enables the generation of higher lift coefficients at lower blowing rates. This

DD FORM 1 JAN 73 1473 EDITION OF 1 NOV 65 IS OBSOLETE

UNCLASSIFIED
SECURITY CLASSIFICATION OF THIS PAGE *(When Data Entered)*

feature enables the test airfoil to equal the performance of single slotted blown airfoils at lower blowing rates therefore reducing the parasitic losses and resulting in higher lift/drag ratios.

A limited study of the ability of the (TRACON) program to predict circulation controlled airfoil performance was conducted. The program failed to provide accurate predictions for the pressure distribution or force coefficients for the airfoil configuration of this study. This study also found that using different geometry smoothing techniques in the region of the slot resulted in large variations in TRACON's performance predictions. The obvious differences between the predicted pressure distribution and the experimental data, leads this author to the conclusion that (TRACON) is still in the developmental stages and should not be used as a design tool.

END

FILMED

3-83

DTIC